# Regulation of long-range planar cell polarity by Fat-Dachsous signaling

**Praveer Sharma[1,2] and Helen McNeill[1,2,*]**

## SUMMARY

Fat (Ft) and Dachsous (Ds) are large cadherins that bind each other and have conserved roles in regulating planar cell polarity (PCP). We quantitatively analyzed Ft-Ds pathway mutant clones for their effects on ommatidial polarity in the *Drosophila* eye. Our findings suggest that the Ft-Ds pathway regulates PCP propagation independently of asymmetric cellular accumulation of Ft or Ds. We find that the Ft effector Atrophin has a position-specific role in regulating polarity in the eye, and that asymmetric accumulation of the atypical myosin Dachs is not essential for production and propagation of a long-range PCP signal. Our observations suggest that Ft and Ds interact to modulate a secondary signal that regulates long-range polarity, that signaling by the Ds intracellular domain is dependent on Ft, and that ommatidial fate specification is genetically separable from long-range signaling.

KEY WORDS: Atrophin, Dachsous, *Drosophila*, Fat, PCP, Polarity

## INTRODUCTION

Development and function of many tissues requires coordination of cellular characteristics along a consistent direction. This coordinate organization is called planar cell polarity (PCP). Most forms of PCP are regulated by two well-conserved pathways: the Frizzled(Fz)/PCP and the Fat (Ft)-Dachsous (Ds) PCP pathway (reviewed by Axelrod, 2009; Goodrich and Strutt, 2011; Lawrence et al., 2007; Maung and Jenny, 2011; Thomas and Strutt, 2012). Ft and Ds are large cadherins (Bryant et al., 1988; Clark et al., 1995; Mahoney et al., 1991), the binding of which is regulated by the kinase Four-jointed (Fj) (Brittle et al., 2010; Ishikawa et al., 2008; Simon et al., 2010). Ds and Fj are expressed in gradients in the eye, regulating Ft activity (Simon, 2004; Yang et al., 2002) (Fig. 1B). Ft, Ds and Fj are also involved in the growth-regulatory Hippo pathway (reviewed by Grusche et al., 2010; Halder and Johnson, 2011; Lawrence et al., 2008; Staley and Irvine, 2012). A crucial question is how the orientation of neighboring cells is established and propagated across a tissue. Analysis of clones of cells lacking *ft*, *ds* or *fj* reveals that mutant tissue inside clones and wild-type tissue adjacent to clones has altered polarity (Casal et al., 2002; Casal et al., 2006; Fanto et al., 2003; Ma et al., 2003; Rawls et al., 2002; Strutt and Strutt, 2002; Yang et al., 2002). The reorganization of polarity in wild-type tissue, called domineering non-autonomy (Krasnow et al., 1995; Vinson and Adler, 1987), can propagate over many cell lengths, indicating that the Ft-Ds pathway has a role in communicating polarity information across a tissue.

Recent studies have revealed that Ft, Ds and the atypical myosin Dachs (D) are asymmetrically distributed (Ambegaonkar et al., 2012; Bosveld et al., 2012; Brittle et al., 2012; Mao et al., 2006; Rogulja et al., 2008). D localization redistributes several cells away from a border of Ds or Fj expression (Ambegaonkar et al., 2012; Bosveld et al., 2012; Brittle et al., 2012; Mao et al., 2006; Mao et al., 2011). These data, along with previous studies, have led to a model in which polarity information is propagated from cell to cell by polarized distribution of Ft and Ds, which in turn reorganizes Ft, Ds and D in adjacent cells (Casal et al., 2006; Ma et al., 2003; Matakatsu and Blair, 2006; Strutt and Strutt, 2002; Yang et al., 2002).

An alternative model to explain the propagation of polarity from Ft- and Ds-expressing cells is that Ft-Ds binding leads to production of a second signal, which is responsible for the propagation of polarity. The finding that the cytoplasmic domain of Ft binds to the transcriptional co-repressor Atrophin (Atro) led to the proposal that this second signal is transcriptionally regulated by Ft activity (Fanto et al., 2003). Loss of either *ft* or *atro* leads to increased expression of *fj*, providing a potential mechanism for regulation of PCP.

We reasoned that quantitative analysis of polarity disruptions caused by mutant clones of *ft*, *ds* and *atro* could provide insight into the mechanisms underlying the propagation of polarity, and allow us to distinguish between these models. Using these analyses, we show that asymmetric subcellular localization of Ft and Ds cannot account for the propagation of polarity in the *Drosophila* eye. We further show that the cytoplasmic domains of Ft and Ds can generate a signal that can propagate across a tissue independently of changes in Ft, Ds or D localization. We demonstrate that *atro* regulates polarity only in regions near the equator, indicating that other, as yet unknown polarity regulators mediate Ft signaling in polar regions. We show that loss of D does not block the propagation of polarity defects, and that increased expression of *fj* cannot account for polarity disruptions caused by loss of *ft* or *atro*. These data support a model in which long-range polarity propagation in the Ft-Ds pathway is mediated by a second signal regulated by Ft-Ds interactions.

## MATERIALS AND METHODS
### Sample preparation
Clones were generated using FLP/FRT with *ey* or *hs* drivers (Xu and Rubin, 1993) and MARCM (Lee and Luo, 2001). Adult clones were marked by loss of *w⁺* or expression of *UAS-W-RNAi*. Adult eyes were sectioned according to Wolff (Wolff, 2000). Antibody staining of eye discs was carried out after 4% PFA fixation and blocking with 1% BSA. Antibodies used were rat α-Ft (1:1000), rabbit α-Ds (1:1000), rat α-Bar (1:100), mouse α-Elav (DSHB, 1:1000) and mouse α-β-gal (Promega, 1:1000).

[1]Samuel Lunenfeld Research Institute, Mount Sinai Hospital, Toronto, ON M5G 1X5, Canada. [2]Department of Molecular Genetics, University of Toronto, Toronto, ON M5S 1A8, Canada.

*Author for correspondence (mcneill@lunenfeld.ca)
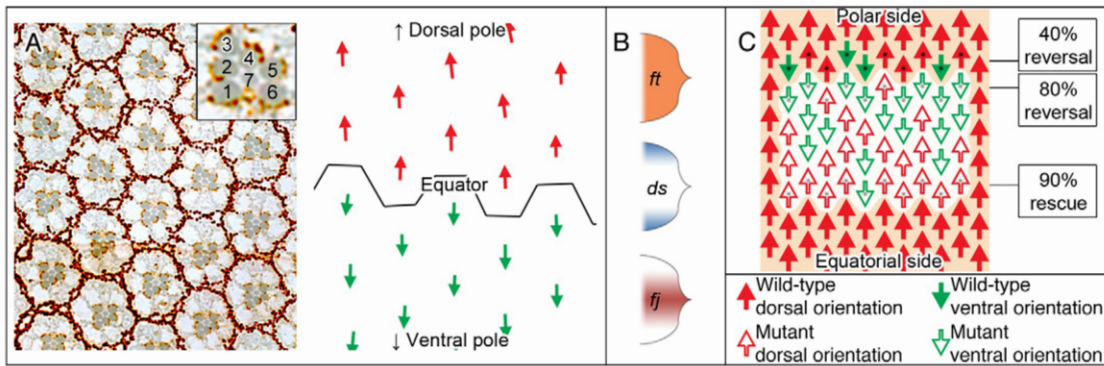
**Fig. 1. Organization of planar polarity in the *Drosophila* eye.** (**A**) Polarity in the *Drosophila* eye. Dorsal ommatidia are marked with red arrows, and ventral ommatidia with green arrows. The dorsoventral midline is the equator, and the opposite ends of the eye are the poles. (**B**) *fat* (*ft*) is expressed evenly throughout the eye disc, as is *atrophin* (*atro*). *dachsous* (*ds*) is expressed highly at the poles, and less around the equator. *four-jointed* (*fj*) has a reverse gradient. (**C**) An example of polarity quantification. This clone has 40% polarity reversal outside the polar border of the clone, 80% reversal inside the polar border and 90% rescue (i.e. normal polarity) inside the equatorial border. Ommatidia that are dorsally oriented are represented as red arrows; those that are ventrally oriented are represented as green arrows. Ommatidia in which both R3 and R4 are wild type are represented as solid arrows; all others are represented as hollow arrows.

## Fly stocks

The following stocks were used: *ft$^{G-rv}$ FRT40. ft$^{fd}$ FRT40. ds$^{38k}$ FRT40* (from David Strutt, University of Sheffield, UK); *ds$^{38k}$ ft$^{G-rv}$ FRT40. ds$^{UAO71}$ ft$^{G-rv}$ FRT40. atro$^{35}$ FRT80. atro$^{e46}$ FRT80* (Manolis Fanto, King's College London, UK). *GFP FRT40. GFP FRT80. GFP FRT40;UAS-FtΔECD* (Seth Blair, University of Wisconsin, Madison, WI, USA); *GFP FRT40;UAS-DsΔECD* (Seth Blair); *GFP FRT40;UAS-fz-RNAi* (TRiP, Boston, MA, USA); *GFP FRT40;UAS-ds-RNAi* (TRiP); *GFP FRT40;UAS-atro-RNAi* (C.-C. Tsai, Rutgers University, Piscataway, NJ, USA); *d$^{GC13}$ FRT40* [Ken Irvine (Rutgers University, Piscataway, NJ, USA) and David Strutt]; *ft$^{G-rv}$ d$^{GC13}$ FRT40* (Ken Irvine and David Strutt); *fat2$^{58D}$ FRT80* (Christian Dahmann, MPI-CBG, Dresden, Germany); *ft$^{G-rv}$ FRT40;UAS-FtΔECD; ft$^{G-rv}$ FRT40;UAS-fz-RNAi; ds$^{38k}$ FRT40;UAS-DsΔECD; ft$^{G-rv}$ FRT40;UAS-DsΔECD; ds$^{38k}$ ft$^{G-rv}$ FRT40;UAS-DsΔECD; ds$^{38k}$ FRT40;UAS-fz-RNAi; ds$^{38k}$ FRT40;UAS-atro-RNAi; ft$^{G-rv}$ FRT40 fj$^{D1}$; ds$^{38k}$ FRT40 fj$^{D1}$; ds$^{38k}$ ft$^{G-rv}$ FRT40 fj$^{D1}$; fj$^{D1}$;atro$^{35}$ FRT80; GFP FRT40 fj$^{D1}$; fj$^{D1}$;GFP FRT80; ft$^{G-rv}$ FRT40;fat2$^{58D}$ FRT80; ds$^{38k}$ FRT40;fat2$^{58D}$ FRT80; GFP FRT40;fat2$^{58D}$ FRT80; ser-lacZ.II-9.5* (Maria Dominguez, Universidad Miguel Hernández – CSIC, Alicante, Spain); and *ft$^{G-rv}$ FRT40;ser-lacZ. ds$^{38k}$ FRT40;ser-lacZ. ds$^{38k}$ ft$^{G-rv}$ FRT40;ser-lacZ.*

## Polarity determination

As ommatidial polarity determination occurs through photoreceptor R3/4 fate determination (Cooper and Bray, 1999; Fanto and Mlodzik, 1999; Fanto et al., 2003; Yang et al., 2002; Zheng et al., 1995), and it has been shown that R3/R4 mosaicism can affect ommatidial polarity, we excluded ommatidia that were mosaic for R3/R4 from our analysis of long-range polarity. We considered ommatidia in which R3 and R4 cells were both wild type as wild type for the purpose of long-range polarity establishment, and those in which both were mutant as being genetically mutant, unless otherwise specified. We tested this approach by measuring polarity effects in ommatidia in which all outer photoreceptors were wild type, surrounding *ft*, *ds*, *ds ft* and *atro* mutant clones. These showed similar trends as R3$^+$/R4$^+$ ommatidia (supplementary material Fig. S1), confirming the validity of our analyses. Inside clones, we quantified only entirely mutant ommatidia for polarity analysis. No R3$^+$/R4$^-$ or R3$^-$/R4$^+$ mosaic ommatidia were included in any of our quantification, although we note that R3/R4 mosaic ommatidia tend to have reversed or rescued polarity according to their location in the clone, similar to fully mutant ommatidia (supplementary material Fig. S2).

## Data processing

Images were processed with Adobe Photoshop and statistical analysis was carried out using GraphPad Prism. Comparisons of phenotype strength were done by unpaired *t*-tests, and size- and position-dependence determined by linear regression.

## RESULTS

### *ft* regulates long-distance repolarization independently of changes in Ft localization

To gain insight into the mechanisms underlying polarity propagation, we quantitatively analyzed alterations in polarity that occur in and around Ft-Ds pathway mutant clones (Fig. 1C). We found that *ft$^{G-rv}$* mutant clones cause reversal of polarity in 34% of genetically wild-type ommatidia in the first row of ommatidia outside the polar border of the clone (*n*=40 clones), whereas polarity outside the equatorial border was unaffected (Fig. 2A,C).

Models in which polarity propagation by the Ft-Ds pathway is due to asymmetric distribution of Ft and Ds in one cell promoting asymmetric redistribution of Ds and Ft in adjacent cells predict that: (1) polarity propagation in clones lacking Ft or Ds could only re-orient polarity in one row of cells inside mutant clones; (2) the degree of propagation in wild-type tissue outside clones depends on the relative levels and affinities of Ft and Ds; and (3) inside mutant clones, ommatidia not contacting a wild-type cell should have randomized polarity. To test these predictions, we quantified the degree of polarity disruption inside *ft* clones. If polarity were randomized, quantification should show a polarity distribution of ~50% normally oriented ommatidia and ~50% reverse-oriented ommatidia. A significant departure from this distribution would indicate the presence of polarity signaling in the absence of Ft and Ds redistribution.

We found that inside *ft* clones, 89% of entirely mutant ommatidia in the first row inside the polar border of the clone had reversed polarity (*n*=36 clones) (Fig. 2G). Polarity was almost completely rescued on the equatorial side of *ft* clones, as 93% of entirely mutant ommatidia had normal polarity (*n*=32 clones) (Fig. 2H). The rescue and reversal of polarity were statistically different from the 50% normal/50% reversed polarity distribution expected of randomized ommatidial orientation (both *P*<0.0001). Significantly, and in further contrast to a redistribution model, in the interior of many *ft* clones polarity was normal on the equatorial side and reversed on the polar side over up to four ommatidial rows, in the complete absence of Ft protein (Fig. 2A; supplementary material Fig. S3A). Importantly, these rescue and reversal effects extended to only a limited distance, and polarity was randomized in the middle of large *ft* clones. Another null *ft* allele, *ft$^{fd}$* (Matakatsu and Blair, 2006), showed similar clonal polarity effects (Fig. 2B; supplementary
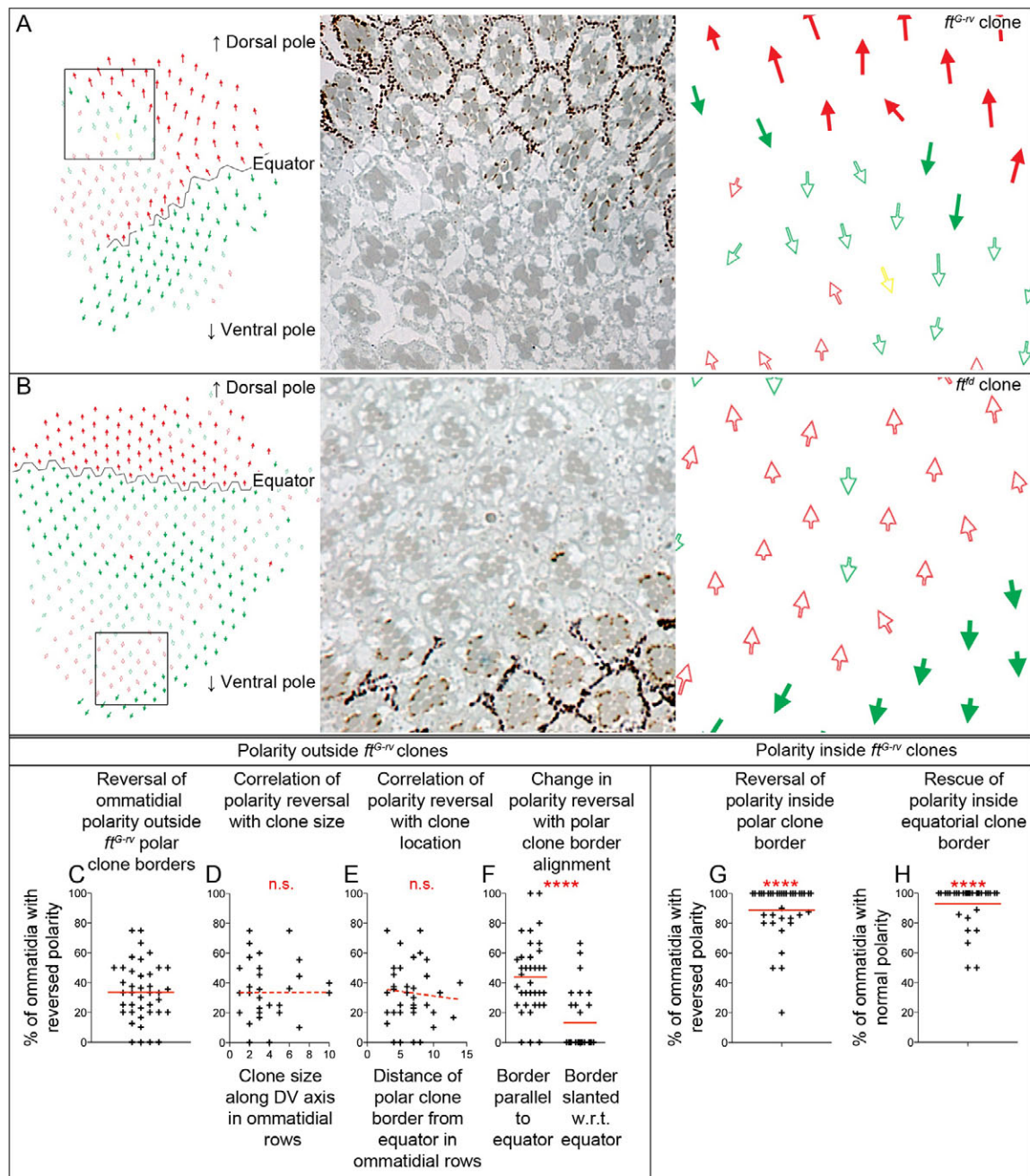
**Fig. 2. Polarity changes propagate from *ft* clone borders.** (**A**) *ft^{G-rv}* mutant clones. The area inside the box is shown in the middle and right panels. Mutant photoreceptors are marked by absence of pigment. Several wild-type ommatidia outside the polar border have reversed polarity. Inside the clone, many mutant ommatidia have reversed polarity on the polar side and normal polarity on the equatorial side. These effects inside the clone extend over many ommatidial rows. (**B**) An eye with *ft^{fd}* mutant clones. Polarity is not disrupted outside this particular clone, but inside the clone many mutant ommatidia have reversed polarity on the polar side and normal polarity on the equatorial side. (C-F) Quantification of polarity effects outside *ft^{G-rv}* clones. Only R3⁺/R4⁺ ommatidia are quantified. (**C**) Polarity is reversed in an average of 34% of ommatidia in the first row outside the polar border (40 clones, 331 ommatidia). There is no x-axis on this and other such scatterplots – data points are distributed for legibility. (**D**) Plot of polarity reversal outside the clone against clone size, measured in ommatidial rows on the dorsoventral axis (36 clones, 274 ommatidia). There is no significant dependence. (**E**) Plot of polarity reversal outside the clone against polar clone border distance from the equator, as measured in ommatidial rows on the dorsoventral axis (37 clones, 282 ommatidia). There is no significant dependence. (**F**) Scatterplots of polarity reversal outside the clone, according to clone border alignment relative to the equator (parallel, 36 clones, 215 ommatidia; slanted, 28 clones, 107 ommatidia). *ft^{G-rv}* clones have significantly different polarity reversal between parallel and slanted clone borders. (G,H) Quantification of polarity effects inside *ft^{G-rv}* clones. Only fully mutant ommatidia are quantified. (**G**) 89% of ommatidia in the first row on the polar side have reversed polarity (36 clones, 153 ommatidia). (**H**) 93% of ommatidia in the first row on the equatorial side have normal polarity (32 clones, 128 ommatidia). (D,E) Deviation from zero (no dependence) of linear regression slope; (F) unpaired *t*-test; (G,H) one sample *t*-test against null hypothesis of randomized polarity (50% reversal). Statistical significance indicators are: $P>0.05$, n.s.; *$P<0.05$; **$P<0.01$; ***$P<0.001$; ****$P<0.0001$. Horizontal bars (solid) indicate mean. Trend lines (dashed) do not indicate significance.

DEVELOPMENT
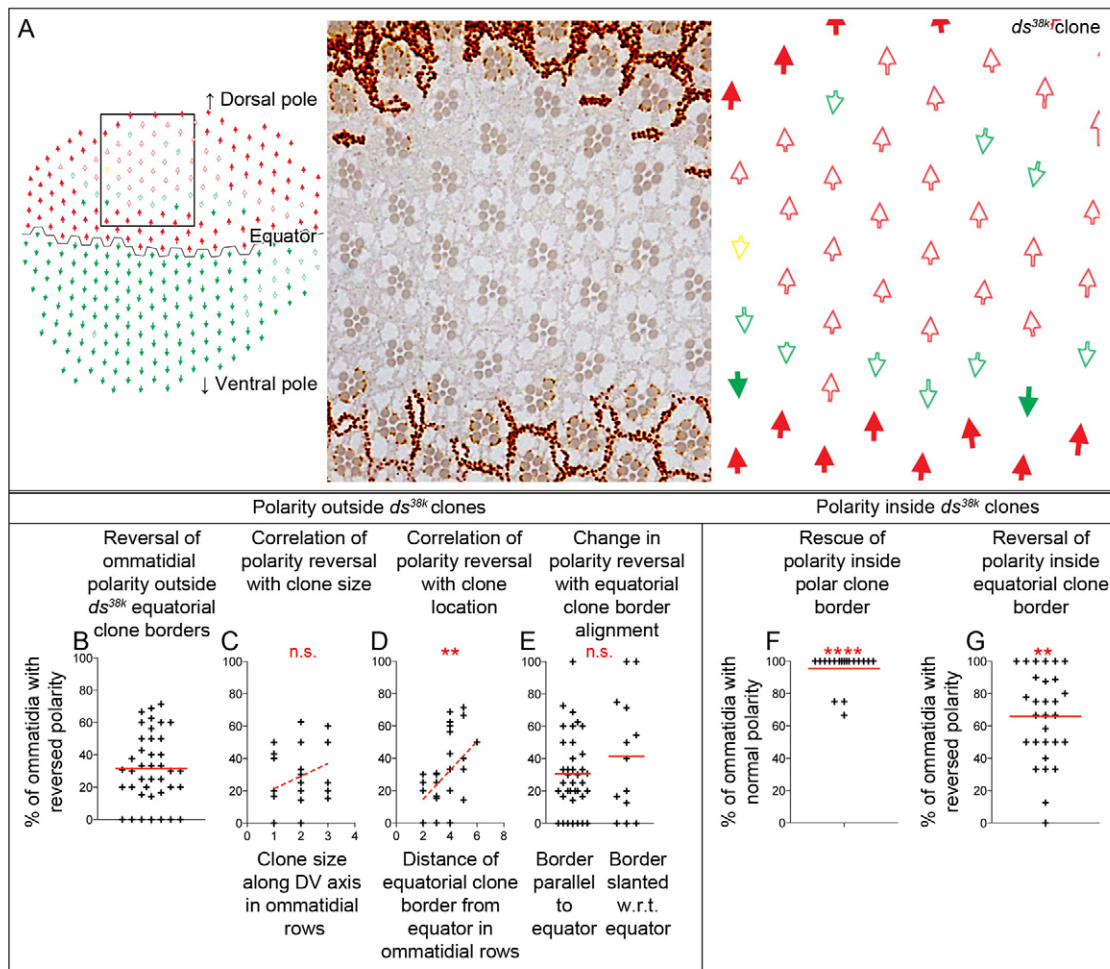
**Fig. 3. Polarity changes propagate from *ds* clone borders.** (**A**) *ds*[38k] mutant clones. Polarity is reversed inside and outside the equatorial border, and rescued inside the polar border. (B-E) Quantification of polarity effects outside *ds*[38k] clones. (**B**) Polarity is reversed in an average of 31% of ommatidia in the first row outside the equatorial border (40 clones, 355 ommatidia). (**C**) Polarity reversals do not vary with clone size (27 clones, 221 ommatidia). (**D**) Polarity reversal increases with distance of clone equatorial border from equator (33 clones, 293 ommatidia). (**E**) Polarity reversal does not vary with clone border alignment relative to equator (parallel, 37 clones, 284 ommatidia; slanted, 13 clones, 71 ommatidia). (F,G) Quantification of polarity effects inside *ds*[38k] clones. (**F**) 95% of ommatidia in the first row on the polar side have normal polarity (36 clones, 153 ommatidia). (**G**) 66% of ommatidia in the first row on the equatorial side have reversed polarity (29 clones, 179 ommatidia). (C,D) Deviation from zero (no dependence) of linear regression slope; (E) unpaired *t*-test; (F,G) one sample *t*-test against null hypothesis of randomized polarity (50% reversal).

material Fig. S4). These data strongly argue that polarity information can propagate ~10-40 cells in the absence of Ft, in contrast to the predictions of an asymmetric redistribution-based model.

### Clonal borders are the source of polarity changes in *ft* clones

We examined whether the degree of polarity reversals caused by *ft* mutant clones varied with clone size along the DV axis and found that it did not – clones that were one to two ommatidial rows in size caused reversals outside clones as often as those that were over five rows in size (Fig. 2D). We also examined effects of DV position, and found that clones near the equator caused reversals as often as those near the poles (*P*=0.63) (Fig. 2E).

Analysis of the shape of clone borders indicated that boundary geometry is crucial in determining the extent of polarity disruption. *ft* clone borders that were parallel to the equator induced more polarity reversals (43%) than clone borders slanted relative to the

equator (10%) (Fig. 2F; supplementary material Fig. S3C), a significant difference (*P*<0.0001). As different alignments of clone boundaries result in different degrees of polarity reversal, we conclude that boundary-specific signaling is likely to be important in the *ft* clonal polarity effect.

### *ds* regulates long-range repolarization independent of changes in Ds levels or localization

We quantitatively analyzed *ds*[38k] clones and found that polarity can also propagate in the absence of Ds (Fig. 3A,B). Polarity reverses in 31% of wild-type ommatidia in the first row of ommatidia outside the equatorial border of *ds* clones (*n*=40 clones). Polarity outside the polar border was unaffected. Polarity information is also transmitted inside *ds* mutant clones. Sixty-six percent of entirely *ds* mutant ommatidia in the first row inside the equatorial border of the clone have reversed polarity (*n*=29 clones) (Fig. 3G), a statistically significant degree of reversal (*P*=0.0046). On the polar
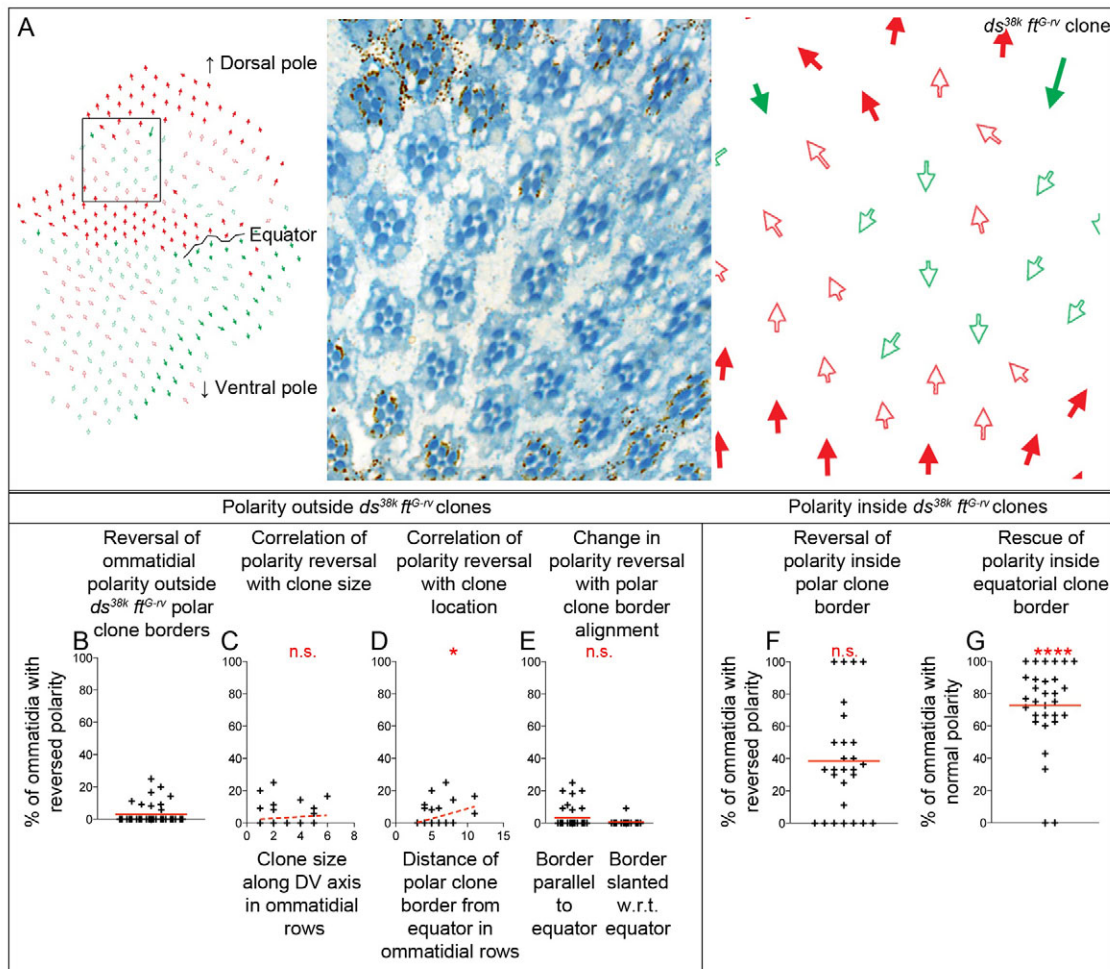
**Fig. 4. Polarity changes are reduced but present at *ds ft* clone borders.** (**A**) An eye with $ds^{38k}\,ft^{G\text{-}rv}$ mutant clones. Several genetically wild-type ommatidia outside the polar border have reversed polarity. Inside the clone, many mutant ommatidia have normal polarity on the equatorial side, but polarity is randomized on the polar side. (B-E) Quantification of polarity effects outside $ds^{38k}\,ft^{G\text{-}rv}$ clones. (**B**) Polarity is reversed in 3% of ommatidia in the first row outside the polar border (40 clones, 288 ommatidia). (**C**) Polarity reversals do not vary with clone size (38 clones, 277 ommatidia). (**D**) Polarity reversal increases slightly with distance of clone equatorial border from equator (36 clones, 267 ommatidia). (**E**) Polarity reversal does not vary with clone border alignment relative to equator (parallel, 26 clones, 211 ommatidia; slanted, 17 clones, 77 ommatidia). (F,G) Quantification of polarity effects inside $ds^{38k}\,ft^{G\text{-}rv}$ clones. (**F**) 62% of ommatidia in the first row on the polar side have reversed polarity, which is statistically similar to randomized polarity (27 clones, 112 ommatidia). (**G**) 73% of ommatidia in the first row on the equatorial side have normal polarity (30 clones, 195 ommatidia). (C,D) Deviation from zero (no dependence) of linear regression slope; (E) unpaired *t*-test; (F,G) one sample *t*-test against null hypothesis of randomized polarity (50% reversal).

side of *ds* clones, 95% of entirely *ds* mutant ommatidia in the first row have normal polarity (*n*=36 clones) (Fig. 3F). As with *ft* mutant clones, polarity rescue extends for many ommatidial rows inside clones, though the reversal effect is weaker (supplementary material Fig. S3B). The degree of polarity reversal caused by *ds* clones does not vary with clone size (*P*=0.09) (Fig. 3C), but does vary with position: *ds* clones near the poles cause more polarity reversals, (*P*=0.007) (Fig. 3D). *ds* levels are higher near the poles, so the difference in levels inside and outside a mutant clone is greater there, which may be responsible for the stronger polarity effect. Unlike *ft* clones, *ds* clones do not show significantly different degrees of reversal along parallel or slanted borders (*P*=0.23) (Fig. 3E). We observed changes in ommatidial orientation inside and outside *ft* and *ds* clonal borders in developing larval eye discs as well (supplementary material Fig. S5). Together, these data indicate that although Ft and Ds are asymmetrically distributed in

wild-type tissue (Ambegaonkar et al., 2012; Brittle et al., 2012), polarity changes in the interiors of *ft* and *ds* mutant clones cannot be accounted for by a chain-reaction propagation of asymmetric Ft-Ds distribution.

*ft* is epistatic to *ds* in R3/4 fate determination (Yang et al., 2002). Quantitative analysis of *ds ft* clones revealed polar non-autonomous polarity effects similar to *ft* clones (Fig. 4A). However, although *ft* clones cause this effect in 34% of ommatidia, only 3% of ommatidia outside *ds ft* clones (*n*=40 clones) have reversed polarity (Fig. 4B). This effect was seen with two strong *ds* mutant alleles, $ds^{38k}\,ft^{G\text{-}rv}$ and $ds^{UAO71}\,ft^{G\text{-}rv}$ (Fig. 4A; supplementary material Fig. S6A), and also when *ds-RNAi* is expressed inside *ds ft* clones (supplementary material Fig. S6C), suggesting that the polarity effects of *ds ft* clones are not due to residual *ds* function. Thus, loss of *ds* largely but not entirely suppresses the polar non-autonomous polarity effects caused by loss of *ft* in clones.

DEVELOPMENT
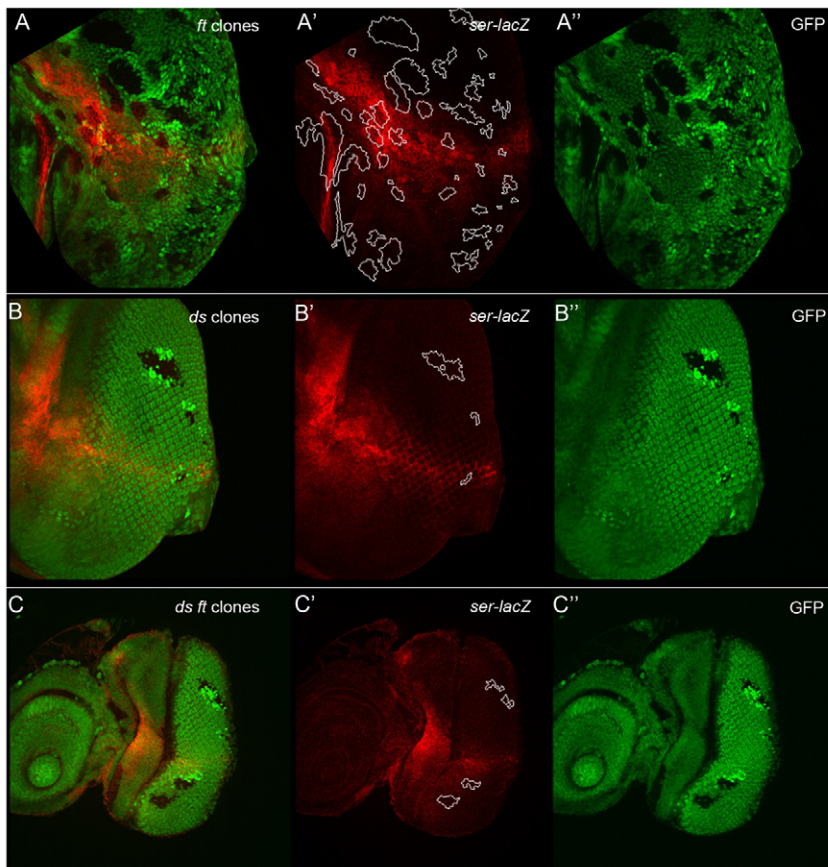
**Fig. 5. Ectopic equators do not form in *ft* or *ds* clones.** Eye discs expressing the equator marker *ser-lacZ*, detected by anti-β-gal staining. No change is observed in Ft-Ds mutant clones, marked by loss of GFP. (**A-A″**) *ft* clones. (**B-B″**) *ds* clones. (**C-C″**) *ds ft* clones.

The polarity reversal observed inside the polar border of *ft* clones does not occur in *ds ft* clones (Fig. 4F). However, 73% of entirely *ds ft* mutant ommatidia in the first row inside the equatorial border have normal polarity, which is statistically different from randomized polarity ($P<0.0001$) (Fig. 4G). Thus, polarity information can be transmitted from clone borders in the absence of both Ft and Ds. The double mutant clonal phenotype is not size dependent ($P=0.52$) (Fig. 4C), and only slightly position dependent, perhaps reflecting the *ds* gradient ($P=0.034$) (Fig. 4D). *ds ft* clones do not show significantly different polarity effects along parallel or slanted borders ($P=0.11$) (Fig. 4E).

It has been suggested that polarity phenotypes associated with *ft* mutant clones are due to generation of an additional equator inside the clones (Rawls et al., 2002), leading to long-distance changes in ommatidial polarity. We did not find changes in the *ser-lacZ* reporter (Fig. 5), which marks regions of equator formation (Bachmann and Knust, 1998; Gutierrez-Aviño et al., 2009), in *ft* or *ds* clones. Furthermore, an ectopic equator would be expected to create a sharp polarity reversal, like the normal equator, in the middle of the clone. However, we find that consistent polarity, whether normal or reversed, is most strongly observed near clone borders, and is increasingly randomized farther inside clones (Fig. 2A, Fig. 3A; supplementary material Fig. S3A,B). We therefore conclude that apparent equators in clone interiors are a consequence of rescue and reversal of polarity at clone borders, and are not true equators, as observed (for example) in Wg pathway clones (Wehrli and Tomlinson, 1998).

Together, these data indicate that accumulation of Ft and Ds at cell borders establishes a polarity signal, and that polarity propagation can occur independently of Ft and Ds.

## Expression of DsΔECD modulates long-range repolarization

Expression of a version of Ft with most of the extracellular domain deleted (FtΔECD) can substantially rescue PCP when expressed ubiquitously in the wing (Matakatsu and Blair, 2006; Matakatsu and Blair, 2012). We found that expression of FtΔECD in clones resulted in rare disruptions in PCP within the clone, and no disruptions outside the clone (Fig. 7C). In contrast to the ability of FtΔECD to rescue polarity in the wing, FtΔECD is unable to rescue *ft* clonal polarity defects in the eye (Fig. 7D). This suggests that the Ft ECD is important for polarity in the eye, possibly via interaction with Ds. Recent work by Zhao et al. (Zhao et al., 2013) found that expression of FtΔECD in fully *ft* mutant eyes also does not rescue polarity, supporting this observation.

Expression of Ds lacking the entire extracellular domain (DsΔECD) in clones resulted in occasional non-autonomous polarity reversals outside the equatorial side of clones (Fig. 7J). This effect, which is qualitatively similar to, but weaker than, the *ds* clone effect, suggests that the Ds intracellular domain (ICD) acts in a dominant-negative manner in non-autonomous polarity signaling. Strikingly, expression of DsΔECD in *ds* clones resulted in polarity disruptions stronger than those of *ds* clones alone, with polarity reversal in 48% of wild-type ommatidia in the first row of ommatidia outside the equatorial border of the clone ($n=18$ clones) (Fig. 7K; supplementary material Fig. S7), significantly stronger than the 31% polarity reversal outside *ds* clones ($P=0.023$).

Importantly, *ft* clones that express DsΔECD do not exhibit the equatorial polarity reversals seen when DsΔECD is expressed in wild-type tissue. They instead behave like *ft* clones with polar reversals (Fig. 7L). Strikingly, *ds ft* clones expressing DsΔECD also
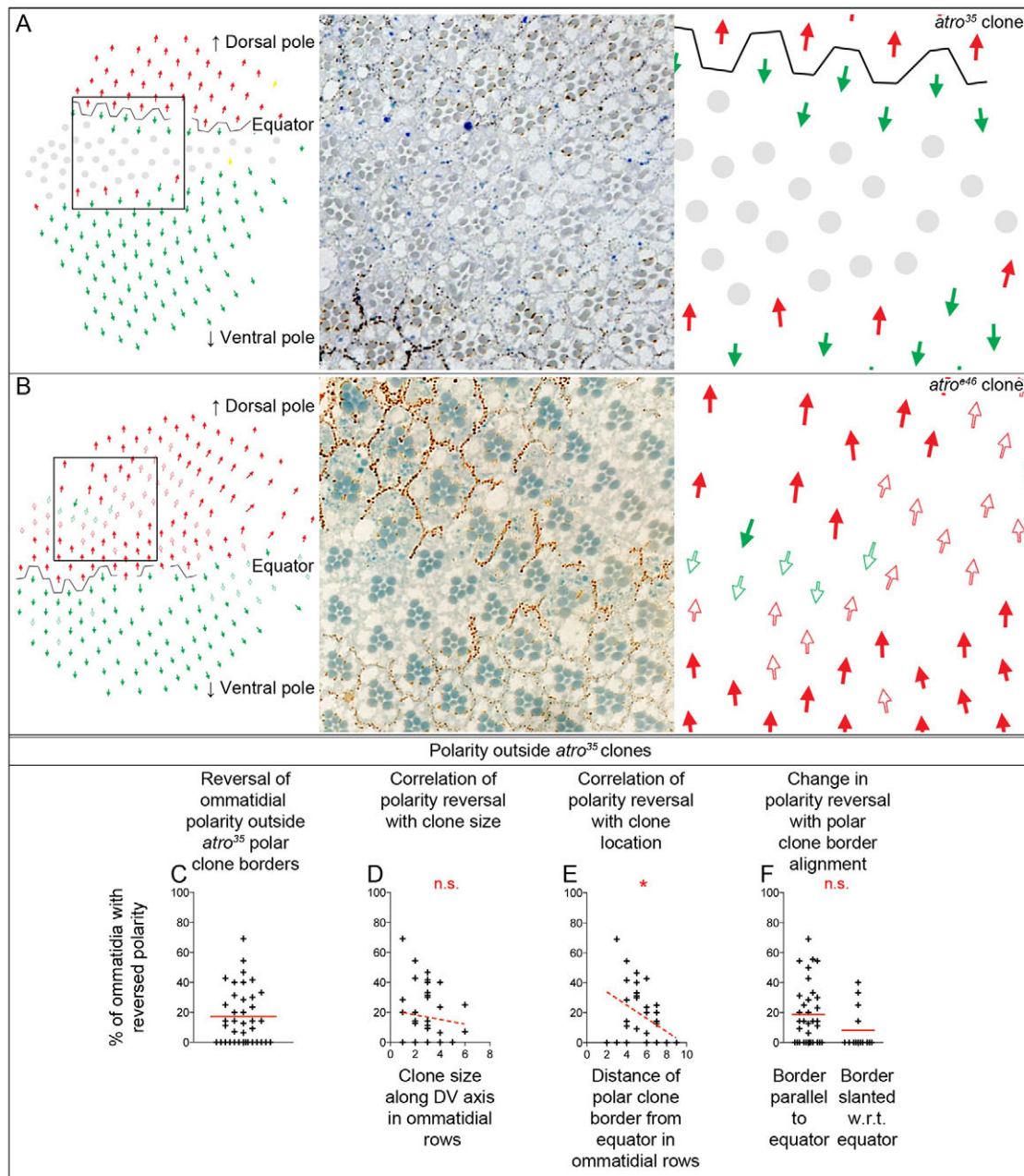
Fig. 6. *atro* primarily regulates polarity near the equator. (**A**) *atro[35]* mutant clones. Several genetically wild-type ommatidia outside the polar border have reversed polarity. (**B**) *atro[e46]* mutant clones. A wild-type ommatidium outside the clone has reversed polarity, while inside the clone, there is both reversal on the polar side and rescue on the equatorial side. (C-F) Quantification of polarity effects outside *atro[35]* clones. (**C**) Polarity is reversed in an average of 17% of ommatidia in the first row outside the polar border (38 clones, 362 ommatidia). (**D**) Polarity reversals do not vary with clone size (38 clones, 362 ommatidia). (**E**) Polarity reversal decreases with distance of clone equatorial border from equator (35 clones, 314 ommatidia). (**F**) Polarity reversal does not vary with clone border alignment relative to equator (parallel, 34 clones, 302 ommatidia; slanted, 14 clones, 66 ommatidia). (D,E) Deviation from zero (no dependence) of linear regression slope; (F) unpaired *t*-test.

have no polarity defects outside their equatorial borders (Fig. 7M), in contrast to 48% equatorial polarity reversals induced by *ds* clones expressing DsΔECD. Thus, as DsΔECD is unable to bind Ft in neighboring cells, DsΔECD-induced polarity changes must depend on the presence of Ft in *cis*.

## Atro regulates polarity near the equator

What is downstream of Ft-Ds signaling? The transcriptional co-repressor Atro binds to the cytoplasmic domain of Ft, and, like *ft*,

loss of *atro* results in changes in polarity (Erkner et al., 2002; Fanto et al., 2003; Zhang et al., 2002), but no quantitative analysis was previously performed. Quantification of polarity disruptions around *atro[35]* clones showed that 17% of wild-type ommatidia in the first row outside the polar border of *atro* clones have reversed polarity (*n*=38 clones) (Fig. 6A,C). Similarly to *ft* clones, the degree of polarity reversals induced by *atro* clones did not change with clone size (*P*=0.56) (Fig. 6D). However, it did change with clone position: clones near the equator caused more reversals
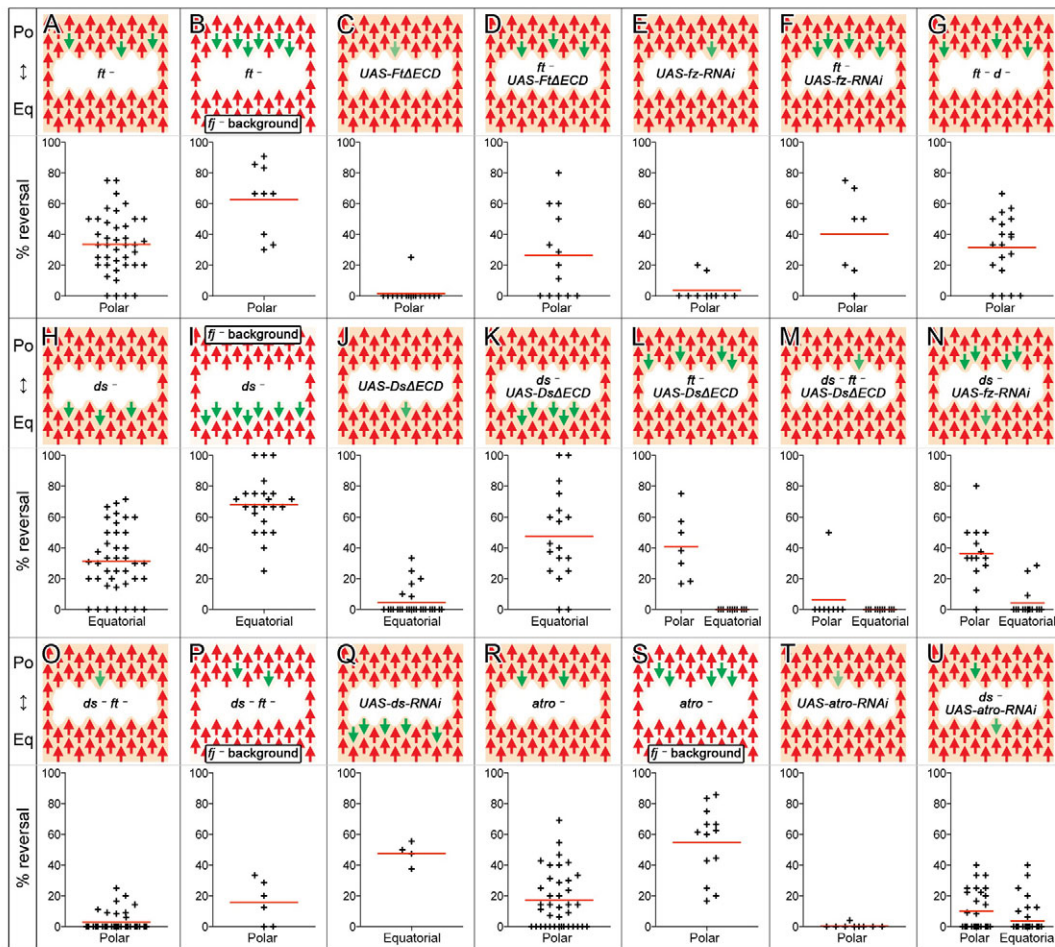
**Fig. 7. Summary of polarity reversal outside mutant clones.** (**A-U**) Diagrams and scatterplots of polarity reversal outside clones. Mutant backgrounds in B, I, P and S are indicated. Strengths of polarity reversal are: (A) *ft⁻* clones, 34% (40 clones, 331 ommatidia); (B) *ft⁻* clones in *fj⁻* background, 63% (9 clones, 65 ommatidia); (C) FtΔECD expression clones, 2% (16 clones, 81 ommatidia); (D) *ft⁻* clones expressing FtΔECD, 26% (13 clones, 71 ommatidia); (E) *fz-RNAi* clones, 4% (10 clones, 58 ommatidia); (F) *ft⁻* clones expressing *fz-RNAi*, 40% (7 clones, 45 ommatidia); (G) *ft⁻ d⁻* clones, 32% (19 clones, 127 ommatidia); (H) *ds⁻* clones, 31% (40 clones, 355 ommatidia); (I) *ds⁻* clones in *fj⁻* background, 68% (23 clones, 112 ommatidia); (J) DsΔECD expression clones, 4% (26 clones, 169 ommatidia); (K) *ds⁻* clones expressing DsΔECD, 48% (18 clones, 120 ommatidia); (L) *ft⁻* clones expressing DsΔECD, 41% polar (7 clones, 71 ommatidia) and 0% equatorial (11 clones, 92 ommatidia); (M) *ds⁻ ft⁻* clones expressing DsΔECD: 6% polar (8 clones, 42 ommatidia) and 0% equatorial (11 clones, 72 ommatidia); (N) *ds⁻* clones expressing *fz-RNAi*, 36% polar (14 clones, 84 ommatidia) and 4% equatorial (15 clones, 114 ommatidia); (O) *ds⁻ ft⁻* clones, 3% (40 clones, 288 ommatidia); (P) *ds⁻ ft⁻* clones in *fj⁻* background, 16% (6 clones, 43 ommatidia); (Q) *ds-RNAi* clones, 48% (4 clones, 40 ommatidia); (R) *atro⁻* clones, 17% (38 clones, 362 ommatidia); (S) *atro⁻* clones in *fj⁻* background, 55% (13 clones, 121 ommatidia); (T) *atro-RNAi* clones, 0.5% (9 clones, 69 ommatidia); (U) *ds⁻* clones expressing *atro-RNAi*, 10% polar (29 clones, 168 ommatidia) and 4% equatorial (44 clones, 302 ommatidia). Statistical comparisons are in supplementary material Table S1.

and those near the poles caused significantly fewer reversals (Fig. 6E).

Strong *atro* alleles cause neurodegeneration in mutant tissue, making polarity inside clones indecipherable. To examine polarity inside *atro* clones, we analyzed a weaker allele: *atro^e46*. Clones of *atro^e46* rarely cause non-autonomous effects, but do cause polar reversal and equatorial rescue inside clones, qualitatively similar to the effect of *ft* clones (Fig. 6B).

Loss of *atro* leads to increased *fj* expression (Fanto et al., 2003). To test whether increased expression of *fj* contributes to polarity disruptions caused by *atro*, we analyzed *atro* clones in *fj^D1*-null background. Strikingly, *atro* clones in *fj⁻* animals caused polarity reversals in 55% of wild-type ommatidia in the first row of ommatidia outside the polar border of the clone (*n*=13 clones) (Fig. 7S), significantly stronger than *atro* clones in a wild-type

background (*P*<0.0001). Thus *fj* is not required for *atro* clones to affect polarity, and in fact loss of *fj* enhances *atro* non-autonomous polarity disruptions.

The degree of polarity reversal does not significantly differ along parallel or slanted *atro* clone borders (*P*=0.08) (Fig. 6F). As *atro* suppresses *ft* expression in the adult eye (Napoletano et al., 2011), one possible mechanism of *atro* activity is through regulating Ft accumulation, promoting polarity disruptions. However, in developing discs, loss of *atro* has no effect on Ft or Ds levels or localization (supplementary material Fig. S8). These data further argue against changes in Ft and Ds localization being responsible for propagation of polarity information, and suggest that a downstream signal establishes polarity.

*ds* and *atro* mutant clones have opposite polarity phenotypes, allowing examination of their epistatic relationship. *ds* and *atro* are

on different chromosomes, so we could not generate double mutant clones. We instead made *ds* clones expressing *atro-RNAi*. These clones caused both polar non-autonomous polarity reversals (more frequently than *atro-RNAi*-only clones), and equatorial non-autonomous polarity reversals (less frequently than *ds* clones (Fig. 7T,U; supplementary material Fig. S9).

## Dachs and Fat2 do not contribute to the long-range repolarization signal

We examined the roles of other polarity regulators in the Ft-Ds pathway. D is an unconventional myosin that acts downstream of Ft (Feng and Irvine, 2007; Mao et al., 2006). D subcellular localization is regulated by Ft and Ds in the wing and eye (Ambegaonkar et al., 2012; Brittle et al., 2012), and loss of *d* suppresses polarity randomization in *ft* and *ds* mutant eyes, probably through its effect on the Hippo pathway (Brittle et al., 2012). However, $d^{GC13}$ mutant flies have extremely mild polarity defects in the eye (Mao et al., 2006) (supplementary material Fig. S10A). Of 45 wild-type ommatidia examined on the polar borders of 11 *d* mutant clones, only one ommatidium had reversed polarity. To examine the contribution of *d* to *ft*-dependent polarity propagation, we examined *ft d* clones and found that they were similar to *ft* clones in their effects on polarity both inside and outside clones (Fig. 7G; supplementary material Fig. S10B). *ft d* clones caused polarity reversals in 31% of wild-type ommatidia in the first row of ommatidia outside the polar border of the clone (*n*=19 clones), similar to the effect of *ft* clones (34% polarity reversal, *P*=0.72), and also display reversal and rescue inside clones. Thus, D does not mediate production and propagation of the Ft-Ds long-range PCP signal in the eye.

*fat2*, the only *ft* paralog in *Drosophila* (Viktorinová et al., 2009), regulates polarization of ovarian follicle cells. We found that neither eyes wholly mutant for $fat2^{58D}$ nor *fat2* mutant clones had polarity defects (supplementary material Fig. S11A,B). Furthermore, the non-autonomous polarity caused by *ft* and *ds* mutant clones was not altered by loss of *fat2* in the background (supplementary material Fig. S11C,D). *fat2*, thus, appears not to be involved in polarity in the *Drosophila* eye.

## Fj dampens long-range repolarization by Ft and Ds

The Golgi-localized kinase Fj acts both upstream and downstream of Ft and Ds (Ishikawa et al., 2008; Strutt et al., 2004; Yang et al., 2002). *fj* expression is negatively regulated by *ft* and *atro*, and positively regulated by *ds* and *d* (Cho et al., 2006; Fanto et al., 2003; Mao et al., 2006; Yang et al., 2002). We therefore examined the role of *fj* in *ft* and *ds* clonal polarity disruptions in the eye.

We found that in a *fj*-null background, polarity reversals caused by *ft* and *ds* mutant clones increased. *ft* clones in a *fj⁻* background caused polar polarity reversals in 63% of wild-type ommatidia (*n*=9 clones) (Fig. 7B), compared with 34% in a wild-type background. *ds* clones in a *fj⁻* background caused equatorial polarity reversals in 68% of wild-type ommatidia (*n*=23 clones) (Fig. 7I), compared with 31% in a wild-type background. Similarly, *ds ft* clones in a *fj⁻* background caused polar polarity reversals in 16% of wild-type (*n*=6 clones) (Fig. 7P), compared with 3% in a wild-type background. Thus, *fj* is not required for non-autonomous polarity of *ft* and *ds* clones, and loss of *fj* strengthens these effects, as with *atro* clones. Interestingly, even though both *ds* and *fj* gradients are absent inside *ds* mutant clones in a *fj⁻* background, there is extensive rescue and reversal of polarity around clone borders (supplementary material Fig. S12).

## Interactions of *ft* and *ds* with *fz*

The relationship between The Ft-Ds and Fz/PCP pathways is complex and context dependent (Adler et al., 1998; Aigouy et al., 2010; Casal et al., 2006; Hogan et al., 2011; Ma et al., 2003; Matakatsu and Blair, 2004; Sagner et al., 2012; Strutt and Strutt, 2002; Yang et al., 2002). *ft* clones and *ds* clones expressing *fz-RNAi* had no consistent rescue or reversal of polarity inside clones. Instead, polarity was randomized, with reversed, misrotated and symmetrical ommatidia (supplementary material Fig. S13), similar to *fz* clones (Zheng et al., 1995). Wild-type ommatidia surrounding *ft* and *ds* mutant clones expressing *fz-RNAi* were often misrotated, complicating analysis. However, we detected polarity reversals in wild-type ommatidia on polar borders of both types of clones, characteristic of the *fz* phenotype (Fig. 7E,F,N; supplementary material Fig. S13A-C). Furthermore, we occasionally observed ommatidia with reversed polarity outside equatorial borders of *ds* clones expressing *fz-RNAi*. These ommatidia were also usually misrotated (supplementary material Fig. S13D). Thus, *ds* clones expressing *fz-RNAi* have stronger polarity effects than *fz-RNAi*-only clones, and weaker equatorial polarity effects than *ds* mutant-only clones.

## DISCUSSION

Ft and Ds can regulate each others subcellular localization, and changes in their levels in clones can induce redistribution outside clone boundaries (Ambegaonkar et al., 2012; Bosveld et al., 2012; Brittle et al., 2012; Ma et al., 2003; Matakatsu and Blair, 2004; Strutt and Strutt, 2002). It has recently been proposed that a redistribution cascade may be responsible for long-range polarity propagation (Ambegaonkar et al., 2012; Brittle et al., 2012). A redistribution cascade cannot, of course, occur inside *ft* or *ds* clones, and yet we observe very strong polarity reorganization well inside these clones. This can only occur if the long-range signaling is occurring through something other than Ft or Ds redistribution. Surprisingly, we find that polarity propagation extends much further in the absence of Ft or Ds, than in wild-type tissue. In *ft* and *ds* clones, rescue or reversal of polarity can in some cases extend to a distance of approximately four ommatidial rows or ~40 cells along the DV axis. The increased range of polarity reversals in the absence of Ft or Ds suggest that the normal distribution of Ft and Ds outside the clone provides a signal that counteracts and dampens the polarity propagation from the clone border. Thus, although the normal asymmetric distribution of Ft and Ds could play a role in creating or orienting the polarity signal, it is not necessary for transmission of the signal.

One surprising result was that ommatidia along borders of *ft* mutant clones that are parallel to the equator are more likely to be reversed than those along slanted borders. What is the basis of this difference? We speculate that this is due to different degrees of accumulation of Ft-Ds interactions at parallel and slanted borders. In the interior of a *ft* clone, Ds is diffusely distributed. At the border of the *ft* clone, all available Ds redistributes to bind Ft in wild-type cells touching the clone (Ma et al., 2003; Simon et al., 2010; Strutt and Strutt, 2002). In *ft* clones that have a border that spreads over several cell diameters along the AP axis, parallel to the equator, this causes redistribution of Ds to only one cell border along the DV axis. Along slanted borders, by contrast, Ds redistribution dissipates over both DV and AP sides of the cell, reducing the degree of accumulation (Fig. 8).

We also examined the effects of expression of FtΔECD and DsΔECD on non-autonomous polarity outside clones. We saw only subtle changes in polarity upon expression of FtΔECD. However, we saw clear non-autonomous polarity effects upon clonal
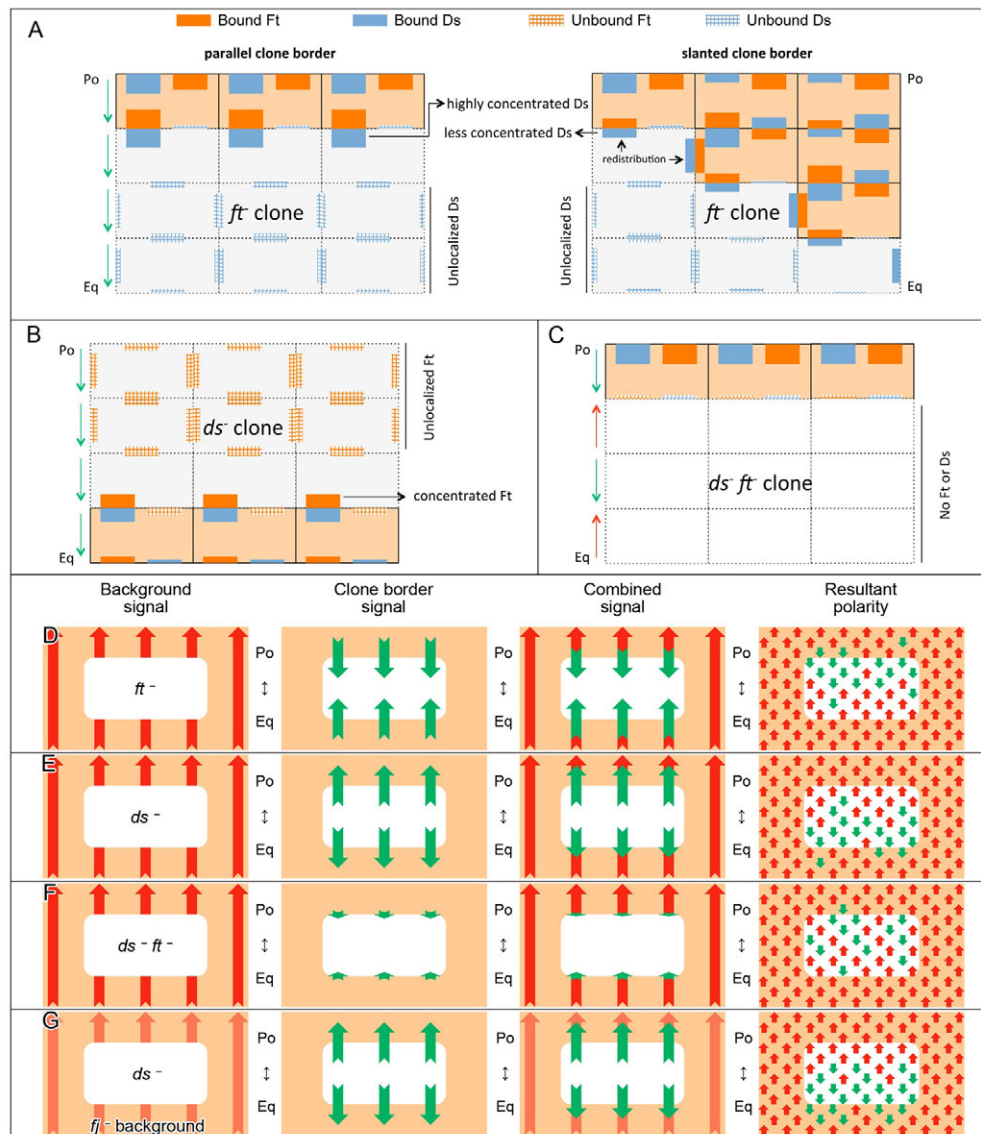
**Fig. 8. A model for Ft-Ds polarity signaling in the eye.** (**A**) Ds accumulates on the borders of *ft* clones, leading to aberrant polarity signal and reversal of polarity on the polar border. On a slanted border, Ds accumulation is redistributed to both sides of cells, leading to a weaker aberrant signal and hence fewer polarity reversals. (**B**) Ft accumulates on the borders of *ds* clones, leading to aberrant polarity signal and reversal of polarity on the equatorial border. (**C**) There is no accumulation of Ft or Ds on a *ds ft* clone border. The aberrant polarity signal is weak, and few polarity reversals occur. (D,E) Polarity inside the clone is established by aberrant polarity signal from clone borders, which can extend to several ommatidial rows. Polarity outside the clone is established by a combination of the aberrant clone border signal and the background polarity signal generated by wild-type tissue. (**D**) *ft* clones cause polar reversals and equatorial rescue. (**E**) *ds* clones cause equatorial reversals and polar rescue. (**F**) *ds ft* clones cause a small amount of equatorial rescue, and very few polar reversals. Polarity is largely randomized inside clones. (**G**) Loss of *fj* weakens the background polarity signal, allowing aberrant signaling from the *ds* clone border to reorganize polarity more extensively.

expression of DsΔECD. Surprisingly, this caused a polarity change qualitatively similar to loss of *ds* in clones, suggesting that DsΔECD had a dominant-negative effect on polarity signaling. Importantly, DsΔECD signals in a Ft-dependent manner, as equatorial polarity disruptions are lost in *ft* clones. As there is no extracellular domain of Ds in DsΔECD, this suggests that Ds ICD interacts with Ft ICD in *cis* to regulate non-autonomous polarity propagation.

Why do *ds ft* clones cause polarity reversals that are a weak version of those caused by *ft* clones? *ft* and *ds* single mutant clones cause strong accumulation of Ds or Ft, respectively, in mutant cells just inside the clone border. In *ds ft* double mutant clones, however,

there would be no such strong accumulation at the border (Fig. 8). There is only loss of signal within clones, which causes milder polarity disruptions.

Why are the border effects of *ft* and *ds* clones opposite in orientation? We speculate that Ft-Ds heterodimers form both in *cis* (in the same cell) and in *trans* (with neighboring cells). In wild-type cells, both *cis* and *trans* forms exist. However, inside *ft* clones, although the Ds protein in a *ft*^{−/−} cell can bind to Ft in adjacent cells, it cannot form a *cis* heterodimer. Similarly, in *ds* clones, although Ft can bind to Ds in adjacent cells, that Ft molecule has no Ds cytoplasmic domain to bind it in *cis*. We propose that the signals

produced upon Ft-Ds binding are affected by both *cis* and *trans* interactions. This difference in signaling by *cis* and *trans* dimers could lead to differential regulation of the same long-range signaling molecule, or to regulation of two different signaling molecules. Although Ft and Ds are both cadherins, they have very different cytoplasmic domains, suggesting they may transmit information about binding in different ways.

What is downstream of Ft-Ds signaling? The Ds intracellular domain is known to affect Hippo pathway targets in the wing (Matakatsu and Blair, 2012), and is required to receive boundary signals that regulate Hippo targets in the eye (Willecke et al., 2008). However, loss of Hippo pathway genes does not lead to non-autonomous polarity disruptions in clones (Blaumueller and Mlodzik, 2000; Harvey et al., 2003; Tapon et al., 2002; Udan et al., 2003; Wu et al., 2003). Although D localization can change in response to Ds levels (Ambegaonkar et al., 2012; Brittle et al., 2012), we find that *d* clones do not cause non-autonomous polarity disruptions, and *ft d* double mutant clones have similar polarity disruptions to *ft* clones. Thus, D is not a component of polarity signal propagation in the eye.

Atro binds to Ft ICD and *atro* clones qualitatively phenocopy *ft* clones (Fanto et al., 2003) (Fig. 6), suggesting Atro could mediate the Ft-Ds polarity signal. Loss of *atro* does not lead to changes in Ft or Ds levels or localization (supplementary material Fig. S8), indicating that *atro* does not affect polarity by changing Ft-Ds accumulation. Interestingly, we found that *atro* mainly functions near the equator, as loss of *atro* near the poles has little effect. This suggests *atro* functions downstream of Ft and Ds near the equator, with another unidentified polarity regulator acting as a Ft-Ds polarity effector near the poles.

Ds, Ft and Fj interactions have been extensively studied in the *Drosophila* abdomen wing, eye and larval denticles (Ambegaonkar et al., 2012; Bosveld et al., 2012; Brittle et al., 2012; Casal et al., 2002; Casal et al., 2006; Donoughe and DiNardo, 2011; Harumoto et al., 2010; Ma et al., 2003; Repiso et al., 2010; Simon, 2004; Strutt et al., 2004; Yang et al., 2002). However, the effects of loss of *fj* on non-autonomous polarity caused by *ft* and *ds* clones have not been examined. *fj* levels are altered in *ft*, *ds* and *atro* mutant clones (Fanto et al., 2003; Yang et al., 2002). If changes in *fj* levels were essential for change in polarity signaling at *ft*, *ds* or *atro* clone borders, the phenotypes of these clones would be weaker in a *fj⁻* animal. Instead, we found that non-autonomous polarity disruptions of *ft*, *ds* or *atro* clones are enhanced in *fj⁻* animals. Thus, changes in *fj* expression cannot be responsible for their non-autonomous polarity effects. The strengthened polarity effects could be explained in terms of diminution of a standing polarity gradient in the wild-type cells surrounding the clone, as *fj* and *ds* establish complementary and redundant polarity gradients in the eye (Simon, 2004; Zeidler et al., 1999). Loss of *fj* strongly enhances polarity phenotypes of Ft, Ds and Ds-ECD overexpression, consistent with this conclusion (Casal et al., 2006; Simon, 2004; Strutt et al., 2004).

*ds* mutant clones expressing *atro-RNAi* cause both polar and equatorial non-autonomous polarity reversals. Analysis of knockdown phenotypes is complicated, but observation of reversals on both sides suggests some parallel function between *ds* and *atro*. Analysis of *ds* clones expressing *fz-RNAi* suggests a similar relationship between *ds* and *fz*.

To summarize, we observe that: (1) polarity information is transmitted to a large (but not unlimited) distance inside *ft* and *ds* clones; and (2) clone size does not affect phenotype but (3) clone shape affects PCP signal generation. These data, along with previously observed changes in localization of Ft and Ds at clone borders (Ma et al., 2003; Matakatsu and Blair, 2004; Strutt and Strutt, 2002), suggest a model in which polarity signals from clone borders act in concert with changes in signaling inside mutant clones. We propose that normal Ft-Ds signaling, acting in a gradient because of graded *ds* and *fj* expression, results in a graded production of long-distance secondary signal. This creates a standing gradient of polarity information. Inside *ft* and *ds* clones, the gradient of polarity information is reduced or lost. These changes are reinforced by accumulation of Ds or Ft at clone borders. The resultant changes in secondary signal oppose the standing gradient in surrounding wild-type tissue, leading to non-autonomous polarity reversals outside the clone. Inside the clone, with no standing gradient to oppose it, the aberrant signal from clone borders leads to extensive reversal or rescue of polarity.

Though our data strongly supports the existence of a long-range signal, its identity is open to speculation. The Fz/PCP pathway itself is an obvious candidate, but it could be another signaling pathway or an as yet unknown factor. With the current absence of a clear mechanistic link between the Ft-Ds and Fz/PCP pathways, or between these pathways and their downstream polarity effectors, the determination of the secondary signal is an unresolved issue.

Extensive structure-function analysis has identified regions of the intracellular domain of Ft that function in PCP regulation (Matakatsu and Blair, 2012; Pan et al., 2013). However, these works examined wholly mutant tissue. Further studies are needed to address the specific regions of the Ft and Ds intracellular domains essential for regulation of long-range polarity signaling.

It is interesting to consider how the same factors, Ft, Ds and Fj, working towards the same goal, i.e. establishing tissue polarity, appear to work in different ways in different contexts (Casal et al., 2006; Matakatsu and Blair, 2012; Willecke et al., 2008). For example, we found that FtΔECD does not rescue polarity effects of *ft* clones in the eye, unlike in the wing and abdomen (Casal et al., 2006; Matakatsu and Blair, 2006; Matakatsu and Blair, 2012). This suggests that the Ft extracellular domain is important for polarity regulation in the eye, perhaps through binding Ds. In the abdomen, *ds ft* clones have no polarity effects outside clones, whereas there are clear, though limited, polarity disruptions outside *ds ft* clones in the eye. Casal and co-workers argue that Ds and Ft are both needed in the receiving cell to propagate Ft and Ds polarity information in the abdomen (Casal et al., 2006). This may be due to tissue-specific differences in signaling.

Our data support a Ft-Ds signaling model in the *Drosophila* eye wherein different levels of Ft and Ds lead to modulation of a long-range polarity effector that directs further polarity establishment in the eye. Propagation of this signal is independent of changes in the asymmetric distribution of Ft and Ds. In at least part of the eye, this process may be mediated by transduction of Ft-binding information to the nucleus by Atro. Further work is needed to understand the identity of the long-range signal(s), and how Ft and Ds levels and interactions alter signal strength.

### Competing interests statement
The authors declare no competing financial interests.

**Author contributions**
H.M. and P.S. designed the experiments. P.S. conducted the experiments. H.M. and P.S. wrote the manuscript.

**Supplementary material**
Supplementary material available online at
http://dev.biologists.org/lookup/suppl/doi:10.1242/dev.094730/-/DC1

**References**
**Adler, P. N., Charlton, J. and Liu, J.** (1998). Mutations in the cadherin superfamily member gene dachsous cause a tissue polarity phenotype by altering frizzled signaling. *Development* **125**, 959-968.
**Aigouy, B., Farhadifar, R., Staple, D. B., Sagner, A., Röper, J. C., Jülicher, F. and Eaton, S.** (2010). Cell flow reorients the axis of planar polarity in the wing epithelium of Drosophila. *Cell* **142**, 773-786.
**Ambegaonkar, A. A., Pan, G., Mani, M., Feng, Y. and Irvine, K. D.** (2012). Propagation of Dachsous-Fat planar cell polarity. *Curr. Biol.* **22**, 1302-1308.
**Axelrod, J. D.** (2009). Progress and challenges in understanding planar cell polarity signaling. *Semin. Cell Dev. Biol.* **20**, 964-971.
**Bachmann, A. and Knust, E.** (1998). Dissection of cis-regulatory elements of the Drosophila gene Serrate. *Dev. Genes Evol.* **208**, 346-351.
**Blaumueller, C. M. and Mlodzik, M.** (2000). The Drosophila tumor suppressor expanded regulates growth, apoptosis, and patterning during development. *Mech. Dev.* **92**, 251-262.
**Bosveld, F., Bonnet, I., Guirao, B., Tlili, S., Wang, Z., Petitalot, A., Marchand, R., Bardet, P. L., Marcq, P., Graner, F. et al.** (2012). Mechanical control of morphogenesis by Fat/Dachsous/Four-jointed planar cell polarity pathway. *Science* **336**, 724-727.
**Brittle, A. L., Repiso, A., Casal, J., Lawrence, P. A. and Strutt, D.** (2010). Four-jointed modulates growth and planar polarity by reducing the affinity of dachsous for fat. *Curr. Biol.* **20**, 803-810.
**Brittle, A., Thomas, C. and Strutt, D.** (2012). Planar polarity specification through asymmetric subcellular localization of Fat and Dachsous. *Curr. Biol.* **22**, 907-914.
**Bryant, P. J., Huettner, B., Held, L. I., Jr, Ryerse, J. and Szidonya, J.** (1988). Mutations at the fat locus interfere with cell proliferation control and epithelial morphogenesis in Drosophila. *Dev. Biol.* **129**, 541-554.
**Casal, J., Struhl, G. and Lawrence, P. A.** (2002). Developmental compartments and planar polarity in Drosophila. *Curr. Biol.* **12**, 1189-1198.
**Casal, J., Lawrence, P. A. and Struhl, G.** (2006). Two separate molecular systems, Dachsous/Fat and Starry night/Frizzled, act independently to confer planar cell polarity. *Development* **133**, 4561-4572.
**Cho, E., Feng, Y., Rauskolb, C., Maitra, S., Fehon, R. and Irvine, K. D.** (2006). Delineation of a Fat tumor suppressor pathway. *Nat. Genet.* **38**, 1142-1150.
**Clark, H. F., Brentrup, D., Schneitz, K., Bieber, A., Goodman, C. and Noll, M.** (1995). Dachsous encodes a member of the cadherin superfamily that controls imaginal disc morphogenesis in Drosophila. *Genes Dev.* **9**, 1530-1542.
**Cooper, M. T. and Bray, S. J.** (1999). Frizzled regulation of Notch signalling polarizes cell fate in the Drosophila eye. *Nature* **397**, 526-530.
**Donoughe, S. and DiNardo, S.** (2011). dachsous and frizzled contribute separately to planar polarity in the Drosophila ventral epidermis. *Development* **138**, 2751-2759.
**Erkner, A., Roure, A., Charroux, B., Delaage, M., Holway, N., Coré, N., Vola, C., Angelats, C., Pagès, F., Fasano, L. et al.** (2002). Grunge, related to human Atrophin-like proteins, has multiple functions in Drosophila development. *Development* **129**, 1119-1129.
**Fanto, M. and Mlodzik, M.** (1999). Asymmetric Notch activation specifies photoreceptors R3 and R4 and planar polarity in the Drosophila eye. *Nature* **397**, 523-526.
**Fanto, M., Clayton, L., Meredith, J., Hardiman, K., Charroux, B., Kerridge, S. and McNeill, H.** (2003). The tumor-suppressor and cell adhesion molecule Fat controls planar polarity via physical interactions with Atrophin, a transcriptional co-repressor. *Development* **130**, 763-774.
**Feng, Y. and Irvine, K. D.** (2007). Fat and expanded act in parallel to regulate growth through warts. *Proc. Natl. Acad. Sci. USA* **104**, 20362-20367.
**Goodrich, L. V. and Strutt, D.** (2011). Principles of planar polarity in animal development. *Development* **138**, 1877-1892.
**Grusche, F. A., Richardson, H. E. and Harvey, K. F.** (2010). Upstream regulation of the hippo size control pathway. *Curr. Biol.* **20**, R574-R582.
**Gutierrez-Aviño, F. J., Ferres-Marco, D. and Dominguez, M.** (2009). The position and function of the Notch-mediated eye growth organizer: the roles of JAK/STAT and four-jointed. *EMBO Rep.* **10**, 1051-1058.
**Halder, G. and Johnson, R. L.** (2011). Hippo signaling: growth control and beyond. *Development* **138**, 9-22.
**Harumoto, T., Ito, M., Shimada, Y., Kobayashi, T. J., Ueda, H. R., Lu, B. and Uemura, T.** (2010). Atypical cadherins Dachsous and Fat control dynamics of noncentrosomal microtubules in planar cell polarity. *Dev. Cell* **19**, 389-401.

**Harvey, K. F., Pfleger, C. M. and Hariharan, I. K.** (2003). The Drosophila Mst ortholog, hippo, restricts growth and cell proliferation and promotes apoptosis. *Cell* **114**, 457-467.
**Hogan, J., Valentine, M., Cox, C., Doyle, K. and Collier, S.** (2011). Two frizzled planar cell polarity signals in the Drosophila wing are differentially organized by the Fat/Dachsous pathway. *PLoS Genet.* **7**, e1001305.
**Ishikawa, H. O., Takeuchi, H., Haltiwanger, R. S. and Irvine, K. D.** (2008). Four-jointed is a Golgi kinase that phosphorylates a subset of cadherin domains. *Science* **321**, 401-404.
**Krasnow, R. E., Wong, L. L. and Adler, P. N.** (1995). Dishevelled is a component of the frizzled signaling pathway in Drosophila. *Development* **121**, 4095-4102.
**Lawrence, P. A., Struhl, G. and Casal, J.** (2007). Planar cell polarity: one or two pathways? *Nat. Rev. Genet.* **8**, 555-563.
**Lawrence, P. A., Struhl, G. and Casal, J.** (2008). Do the protocadherins Fat and Dachsous link up to determine both planar cell polarity and the dimensions of organs? *Nat. Cell Biol.* **10**, 1379-1382.
**Lee, T. and Luo, L.** (2001). Mosaic analysis with a repressible cell marker (MARCM) for Drosophila neural development. *Trends Neurosci.* **24**, 251-254.
**Ma, D., Yang, C. H., McNeill, H., Simon, M. A. and Axelrod, J. D.** (2003). Fidelity in planar cell polarity signalling. *Nature* **421**, 543-547.
**Mahoney, P. A., Weber, U., Onofrechuk, P., Biessmann, H., Bryant, P. J. and Goodman, C. S.** (1991). The fat tumor suppressor gene in Drosophila encodes a novel member of the cadherin gene superfamily. *Cell* **67**, 853-868.
**Mao, Y., Rauskolb, C., Cho, E., Hu, W. L., Hayter, H., Minihan, G., Katz, F. N. and Irvine, K. D.** (2006). Dachs: an unconventional myosin that functions downstream of Fat to regulate growth, affinity and gene expression in Drosophila. *Development* **133**, 2539-2551.
**Mao, Y., Tournier, A. L., Bates, P. A., Gale, J. E., Tapon, N. and Thompson, B. J.** (2011). Planar polarization of the atypical myosin Dachs orients cell divisions in Drosophila. *Genes Dev.* **25**, 131-136.
**Matakatsu, H. and Blair, S. S.** (2004). Interactions between Fat and Dachsous and the regulation of planar cell polarity in the Drosophila wing. *Development* **131**, 3785-3794.
**Matakatsu, H. and Blair, S. S.** (2006). Separating the adhesive and signaling functions of the Fat and Dachsous protocadherins. *Development* **133**, 2315-2324.
**Matakatsu, H. and Blair, S. S.** (2012). Separating planar cell polarity and Hippo pathway activities of the protocadherins Fat and Dachsous. *Development* **139**, 1498-1508.
**Maung, S. M. and Jenny, A.** (2011). Planar cell polarity in Drosophila. *Organogenesis* **7**, 165-179.
**Napoletano, F., Occhi, S., Calamita, P., Volpi, V., Blanc, E., Charroux, B., Royet, J. and Fanto, M.** (2011). Polyglutamine Atrophin provokes neurodegeneration in Drosophila by repressing fat. *EMBO J.* **30**, 945-958.
**Pan, G., Feng, Y., Ambegaonkar, A. A., Sun, G., Huff, M., Rauskolb, C. and Irvine, K. D.** (2013). Signal transduction by the Fat cytoplasmic domain. *Development* **140**, 831-842.
**Rawls, A. S., Guinto, J. B. and Wolff, T.** (2002). The cadherins fat and dachsous regulate dorsal/ventral signaling in the Drosophila eye. *Curr. Biol.* **12**, 1021-1026.
**Repiso, A., Saavedra, P., Casal, J. and Lawrence, P. A.** (2010). Planar cell polarity: the orientation of larval denticles in Drosophila appears to depend on gradients of Dachsous and Fat. *Development* **137**, 3411-3415.
**Rogulja, D., Rauskolb, C. and Irvine, K. D.** (2008). Morphogen control of wing growth through the Fat signaling pathway. *Dev. Cell* **15**, 309-321.
**Sagner, A., Merkel, M., Aigouy, B., Gaebel, J., Brankatschk, M., Jülicher, F. and Eaton, S.** (2012). Establishment of global patterns of planar polarity during growth of the Drosophila wing epithelium. *Curr. Biol.* **22**, 1296-1301.
**Simon, M. A.** (2004). Planar cell polarity in the Drosophila eye is directed by graded Four-jointed and Dachsous expression. *Development* **131**, 6175-6184.
**Simon, M. A., Xu, A., Ishikawa, H. O. and Irvine, K. D.** (2010). Modulation of fat:dachsous binding by the cadherin domain kinase four-jointed. *Curr. Biol.* **20**, 811-817.
**Staley, B. K. and Irvine, K. D.** (2012). Hippo signaling in Drosophila: recent advances and insights. *Dev. Dyn.* **241**, 3-15.
**Strutt, H. and Strutt, D.** (2002). Nonautonomous planar polarity patterning in Drosophila: disheveled-independent functions of frizzled. *Dev. Cell* **3**, 851-863.
**Strutt, H., Mundy, J., Hofstra, K. and Strutt, D.** (2004). Cleavage and secretion is not required for Four-jointed function in Drosophila patterning. *Development* **131**, 881-890.
**Tapon, N., Harvey, K. F., Bell, D. W., Wahrer, D. C. R., Schiripo, T. A., Haber, D. A. and Hariharan, I. K.** (2002). salvador Promotes both cell cycle exit and apoptosis in Drosophila and is mutated in human cancer cell lines. *Cell* **110**, 467-478.
**Thomas, C. and Strutt, D.** (2012). The roles of the cadherins Fat and Dachsous in planar polarity specification in Drosophila. *Dev. Dyn.* **241**, 27-39.

**Udan, R. S., Kango-Singh, M., Nolo, R., Tao, C. and Halder, G.** (2003). Hippo promotes proliferation arrest and apoptosis in the Salvador/Warts pathway. *Nat. Cell Biol.* **5**, 914-920.

**Viktorinová, I., König, T., Schlichting, K. and Dahmann, C.** (2009). The cadherin Fat2 is required for planar cell polarity in the Drosophila ovary. *Development* **136**, 4123-4132.

**Vinson, C. R. and Adler, P. N.** (1987). Directional non-cell autonomy and the transmission of polarity information by the frizzled gene of Drosophila. *Nature* **329**, 549-551.

**Wehrli, M. and Tomlinson, A.** (1998). Independent regulation of anterior/posterior and equatorial/polar polarity in the Drosophila eye; evidence for the involvement of Wnt signaling in the equatorial/polar axis. *Development* **125**, 1421-1432.

**Willecke, M., Hamaratoglu, F., Sansores-Garcia, L., Tao, C. and Halder, G.** (2008). Boundaries of Dachsous Cadherin activity modulate the Hippo signaling pathway to induce cell proliferation. *Proc. Natl. Acad. Sci. USA* **105**, 14897-14902.

**Wolff, T.** (2000). Histological techniques for the Drosophila eye part II: Adult. In *Drosophila Protocols* (ed. W. Sullivan, M. Ashburner and R.S. Hawley). Cold Spring Harbor, NY: Cold Spring Harbor Laboratory Press.

**Wu, S., Huang, J., Dong, J. and Pan, D.** (2003). hippo encodes a Ste-20 family protein kinase that restricts cell proliferation and promotes apoptosis in conjunction with salvador and warts. *Cell* **114**, 445-456.

**Xu, T. and Rubin, G. M.** (1993). Analysis of genetic mosaics in developing and adult Drosophila tissues. *Development* **117**, 1223-1237.

**Yang, C. H., Axelrod, J. D. and Simon, M. A.** (2002). Regulation of Frizzled by fat-like cadherins during planar polarity signaling in the Drosophila compound eye. *Cell* **108**, 675-688.

**Zeidler, M. P., Perrimon, N. and Strutt, D. I.** (1999). The four-jointed gene is required in the Drosophila eye for ommatidial polarity specification. *Curr. Biol.* **9**, 1363-1372.

**Zhang, S., Xu, L., Lee, J. and Xu, T.** (2002). Drosophila atrophin homolog functions as a transcriptional corepressor in multiple developmental processes. *Cell* **108**, 45-56.

**Zhao, X., Yang, C.-H. and Simon, M. A.** (2013). The Drosophila cadherin Fat regulates tissue size and planar cell polarity through different domains. *Plos One* **8**, e62998.

**Zheng, L., Zhang, J. and Carthew, R. W.** (1995). frizzled regulates mirror-symmetric pattern formation in the Drosophila eye. *Development* **121**, 3045-3055.
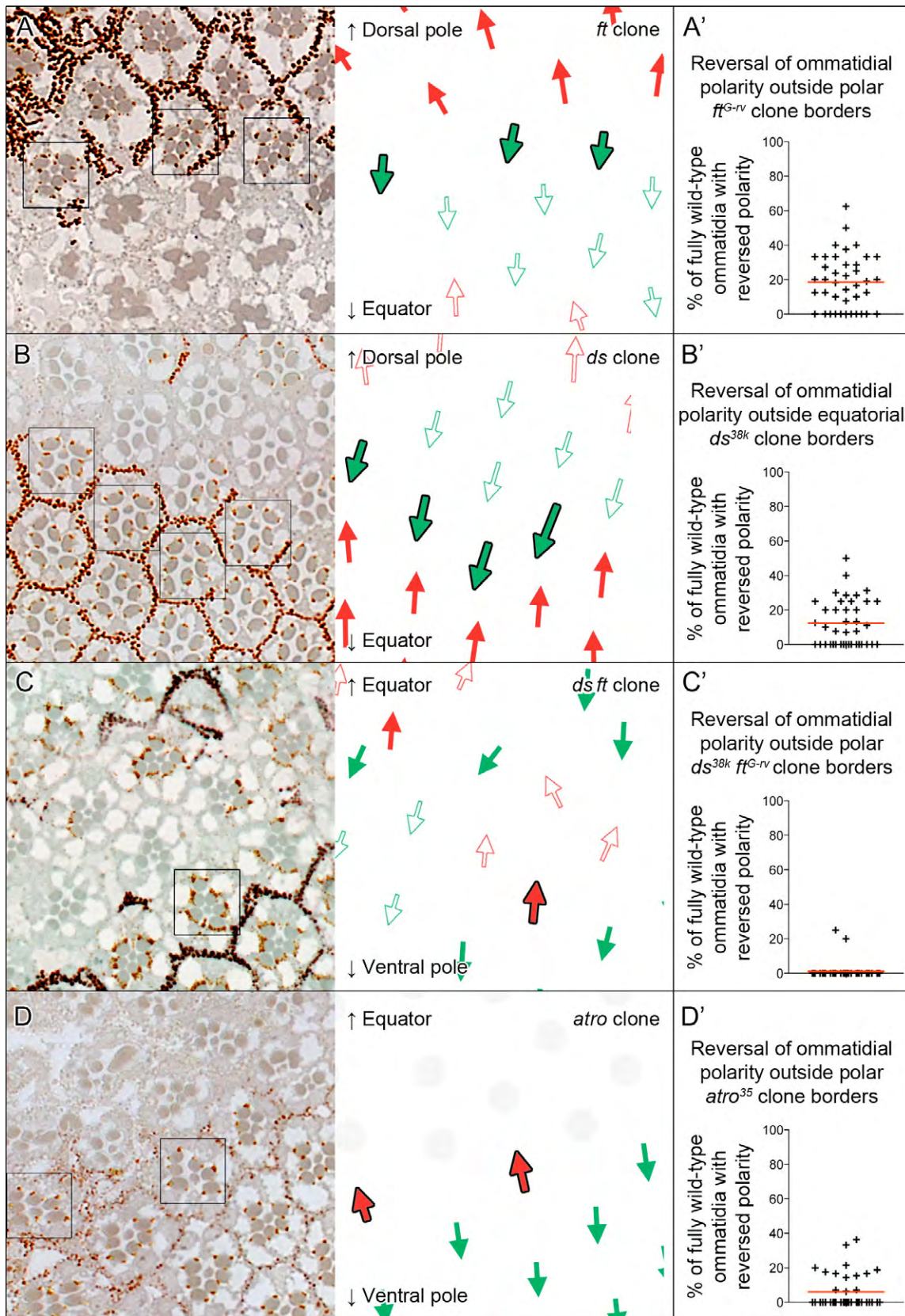
**Fig. S1. Polarity reversals occur in fully wild-type ommatidia on clone borders.** Polarity reversals in ommatidia with at least seven wild-type photoreceptors. In this figure, these fully wild-type ommatidia are enclosed in boxes in the sections, and are represented as solid arrows with a black outline to distinguish them from ommatidia that are R3$^+$/R4$^+$ but mosaic for other photoreceptors, which do not have the black outline. (A,A′) *ft* clones cause polarity reversals in 19% of fully wild-type ommatidia on the polar side (*n*=40 clones/331 ommatidia). (B,B′) *ds* clones cause polarity reversals in 12% of fully wild-type ommatidia on the equatorial side (*n*=40 clones/355 ommatidia). (C,C′) *ds ft* clones cause polarity reversals in 1% of fully wild-type ommatidia on the polar side (*n*=40 clones/288 ommatidia). (D,D′) *atro* clones cause polarity reversals in 6% of fully wild-type ommatidia on the polar side (*n*=38 clones/362 ommatidia).
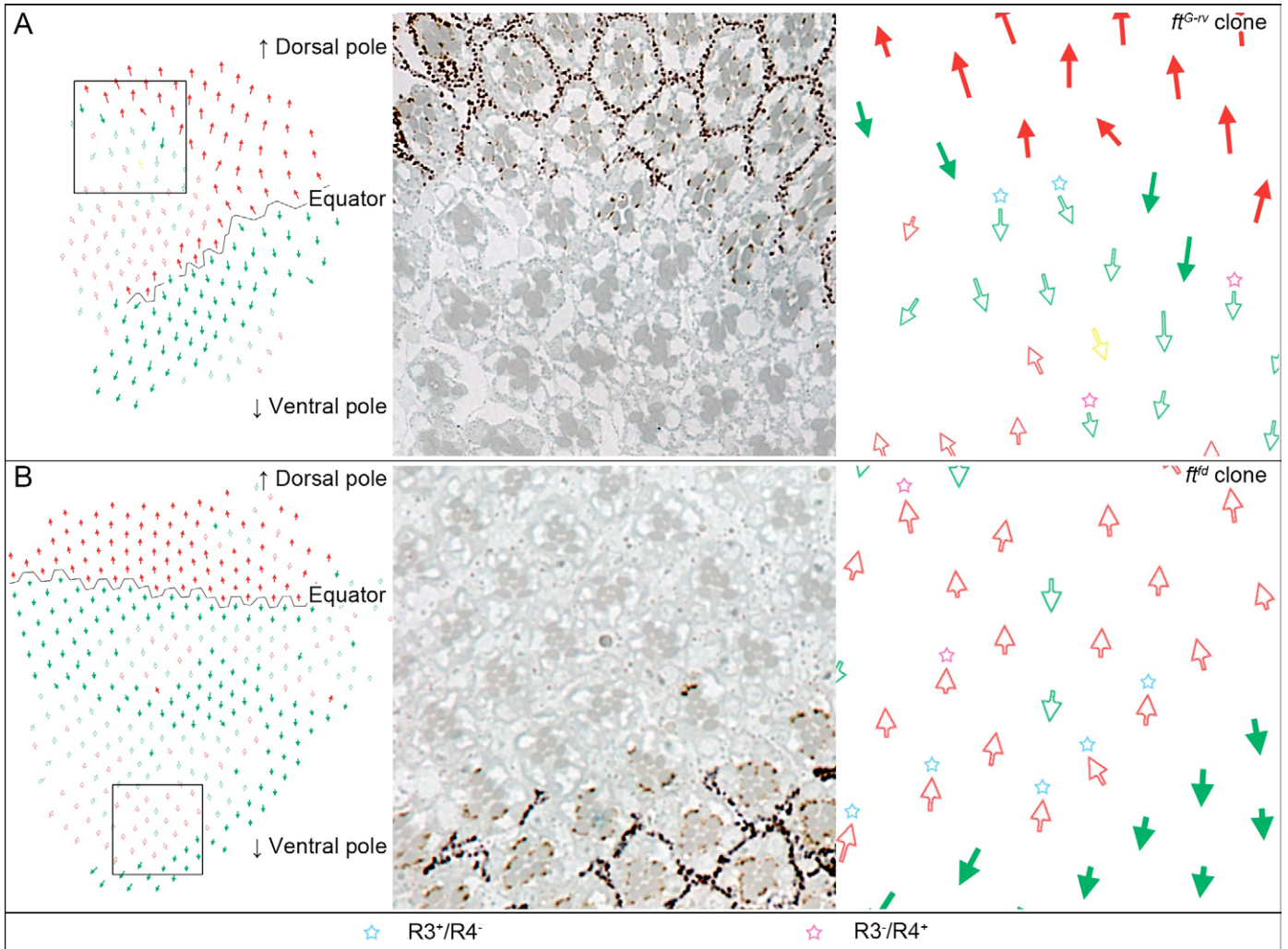
**Fig. S2. R3/R4 mosaic ommatidia behave like fully mutant ommatidia in responding to polarity signals.** R3/R4 mosaic ommatidia are represented with stars over hollow arrows (R3+/R4−: cyan stars, R3−/R4+: magenta stars). (**A**) Mosaic ommatidia on the polar border of a $ft^{G-rv}$ clone have reversed polarity, similarly to their fully mutant neighbors. (**B**) Mosaic ommatidia on the polar border of a $ft^{fd}$ clone have reversed polarity, similarly to their fully mutant neighbors.
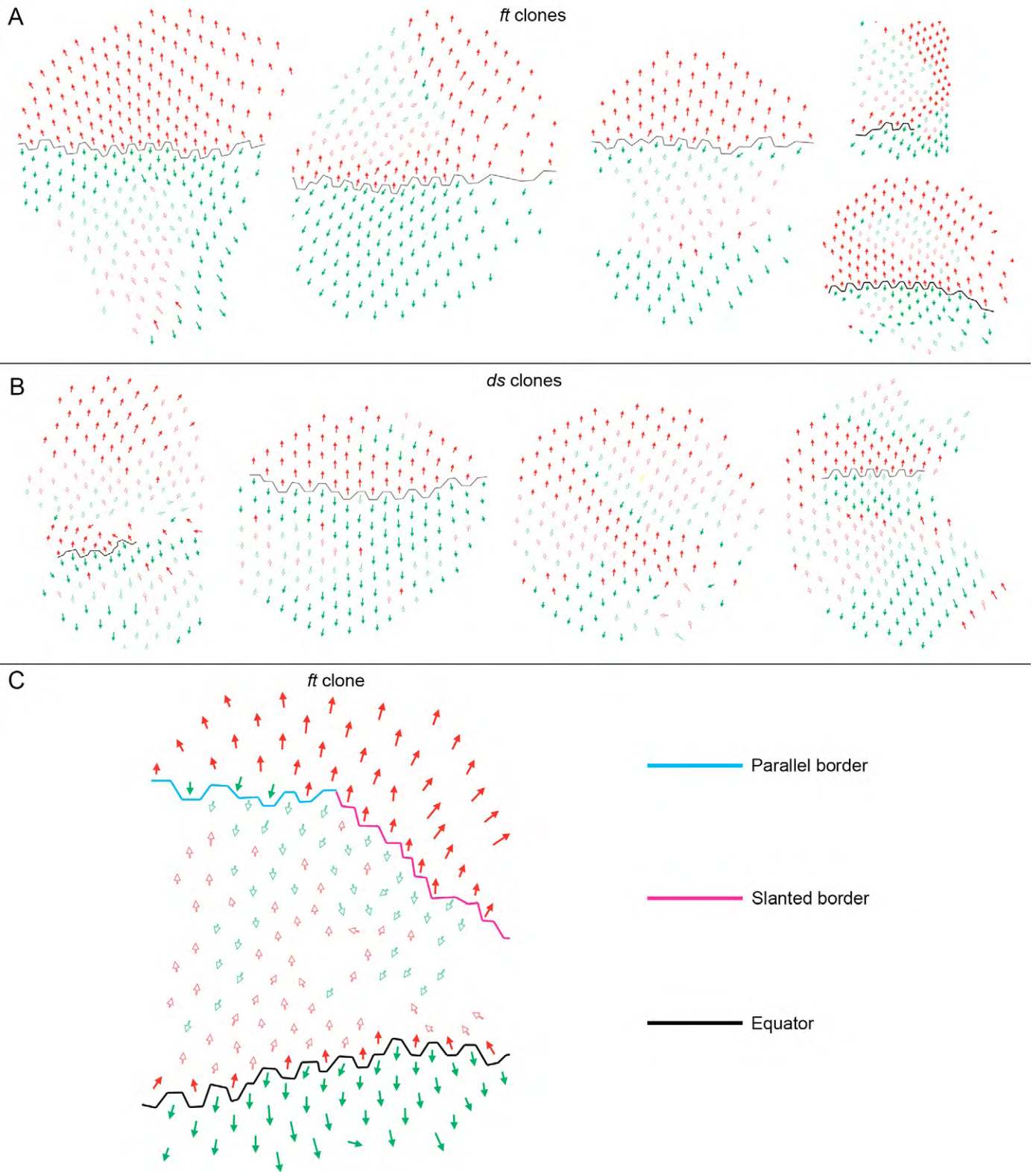
**Fig. S3. Polarity information is transmitted inside *ft* and *ds* clones.** (**A**) *ft* clones have polarity rescued on the equatorial side, and reversed on the polar side. These effects are strongest near the borders and extend up to several rows. In the middle of the clones these effects are weak or non-existent, and polarity is randomized. (**B**) *ds* clones have polarity rescued on the polar side, and reversed on the equatorial side. The reversal effect of *ds* clones is not as strong as that of *ft* clones, and rarely extends past one ommatidial row. However, the rescue effect is strong, and can extend for multiple rows. (**C**) Example of a *ft* clone indicating clone borders parallel (cyan line) and slanted (magenta line) relative to the equator. This clone shows the general trend of parallel borders to have more reversals than slanted borders.
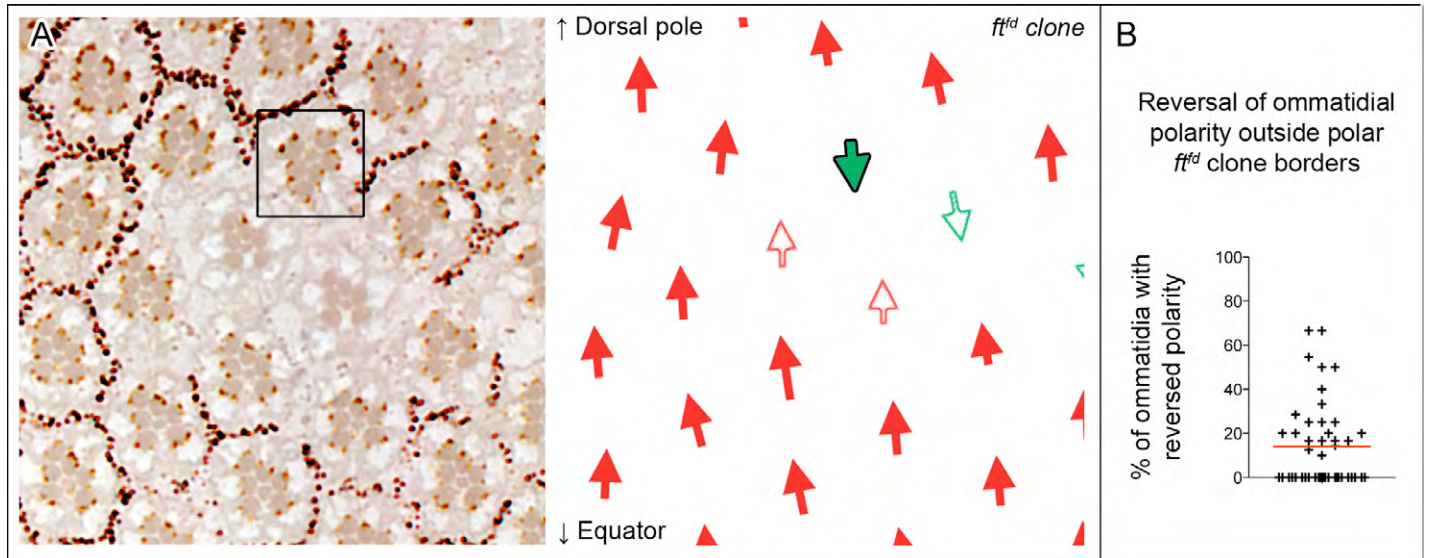
**Fig. S4. *ft^fd* affects polarity similarly to *ft^G-rv*.** *ft^fd* mutant clones cause polarity reversals in the eye qualitatively similar to *ft^G-rv* mutant clones. (**A**) Polarity reversal of an ommatidium with seven wild-type photoreceptors (in box) on the polar side of a *ft^fd* mutant clone. (**B**) Scatterplot of polarity reversals outside polar borders of *ft^fd* clones. The mean strength is 14% (*n*=46 clones).
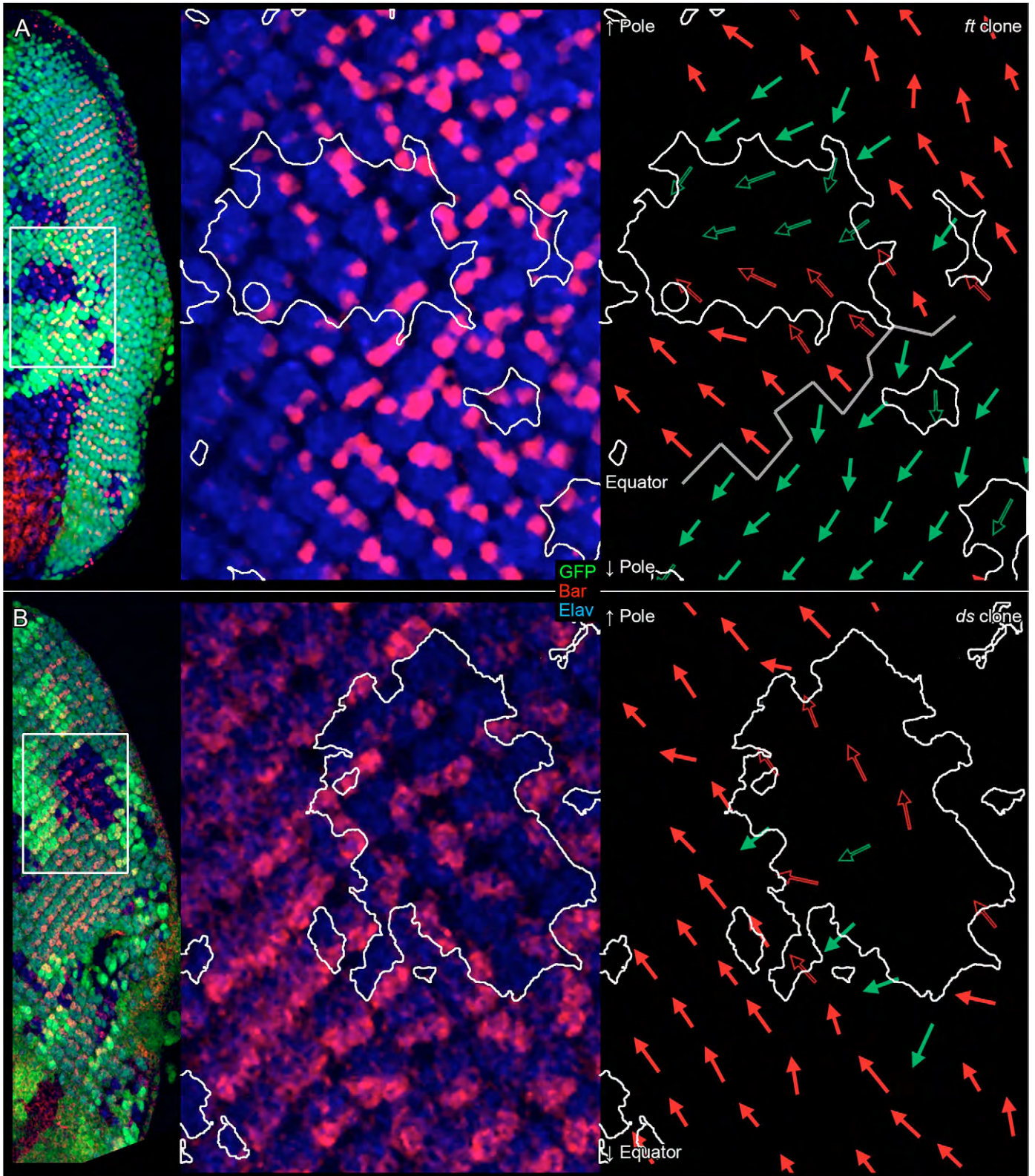
**Fig. S5. Polarity disruptions are evident during development in the eye imaginal disc.** Elav staining marks all photoreceptors, and Bar staining marks photoreceptors 1 and 6. Loss of GFP marks mutant tissue. Mutant tissue is outlined in white in higher magnifications. (**A**) *ft* clones cause polarity disruptions on the polar side of clones. (**B**) *ds* clones cause polarity disruptions on the equatorial side of clones.
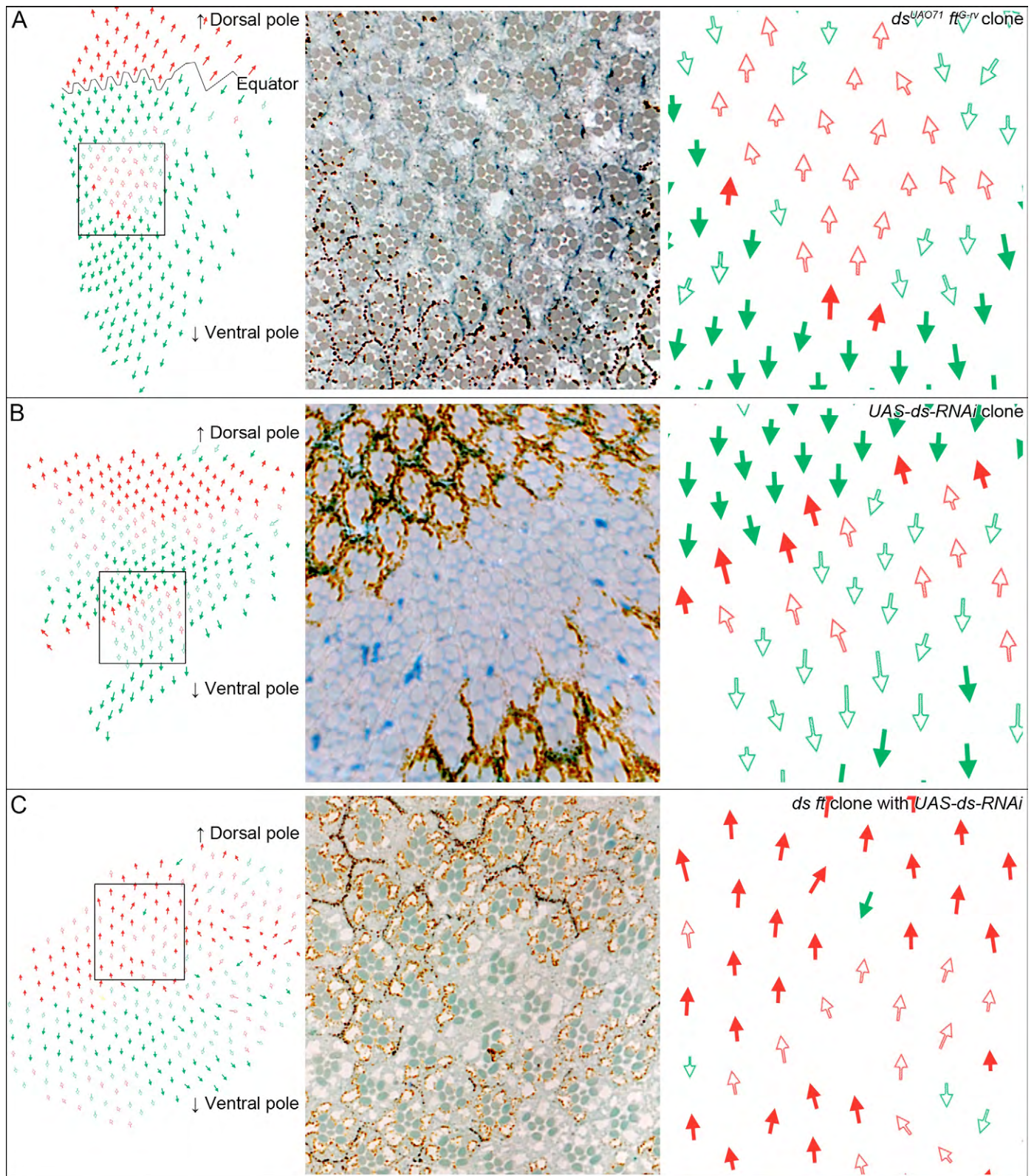
**Fig. S6. Residual *ds* function does not cause *ds ft* clonal polarity effects.** (**A**) *ds^UAO71 ft^G-rv* clones, marked by absence of pigment, show polarity reversals outside clones similarly to *ds^38k ft^G-rv* clones. (**B**) Clones expressing *UAS-ds-RNAi*, marked by absence of pigment, show polarity reversals outside equatorial borders of clones, confirming *ds* knockdown. (**C**) *ds^38k ft^G-rv* clones expressing *UAS-ds-RNAi*, marked by absence of pigment, show polarity reversals outside clones similar to *ds ft* clones not expressing RNAi.
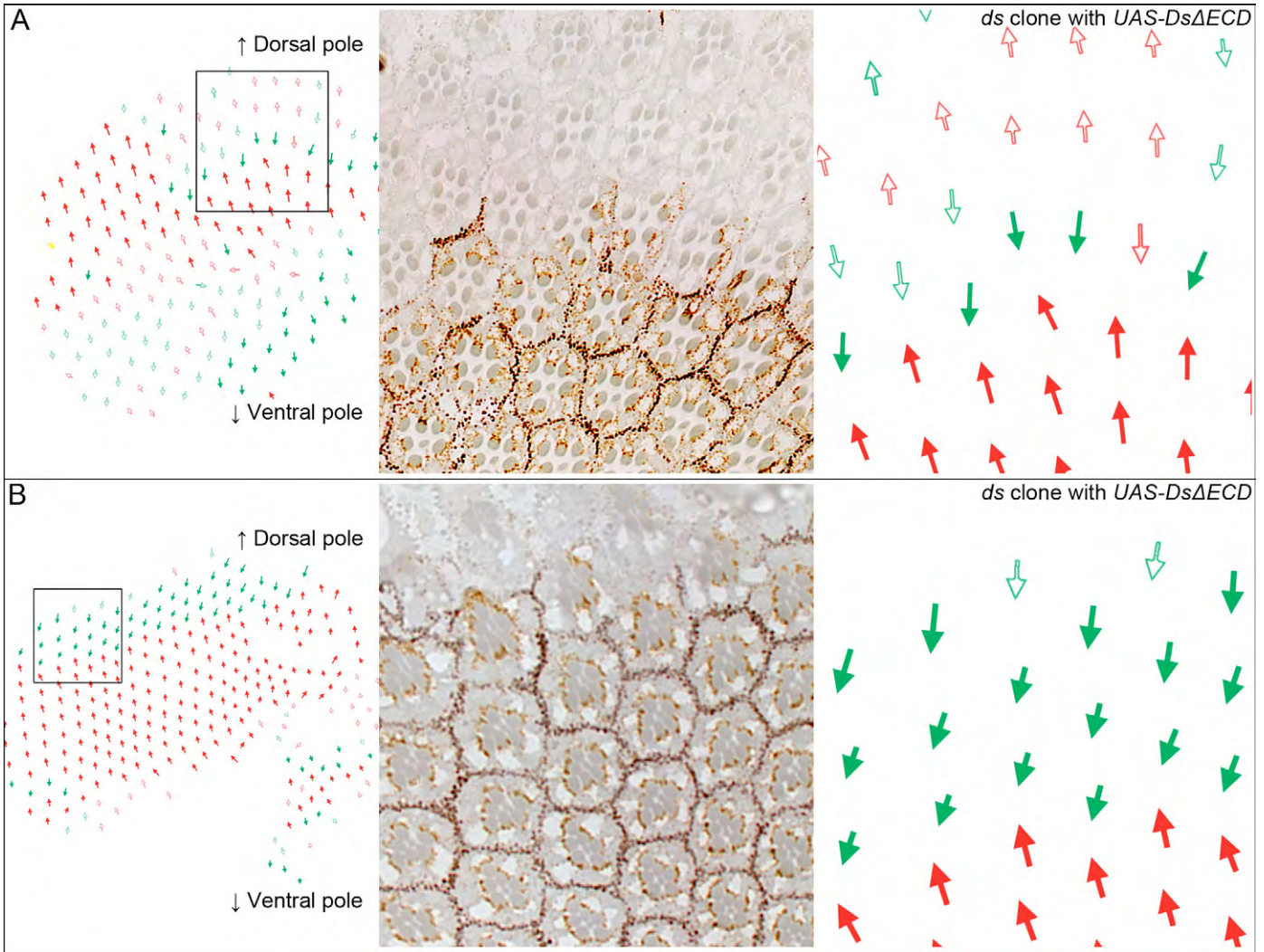
**Fig. S7. Expression of DsΔECD strengthens *ds* clonal polarity effects.** (**A**,**B**) *ds* mutant clones expressing *UAS-DsΔECD*. There is very strong polarity reversal outside equatorial borders.
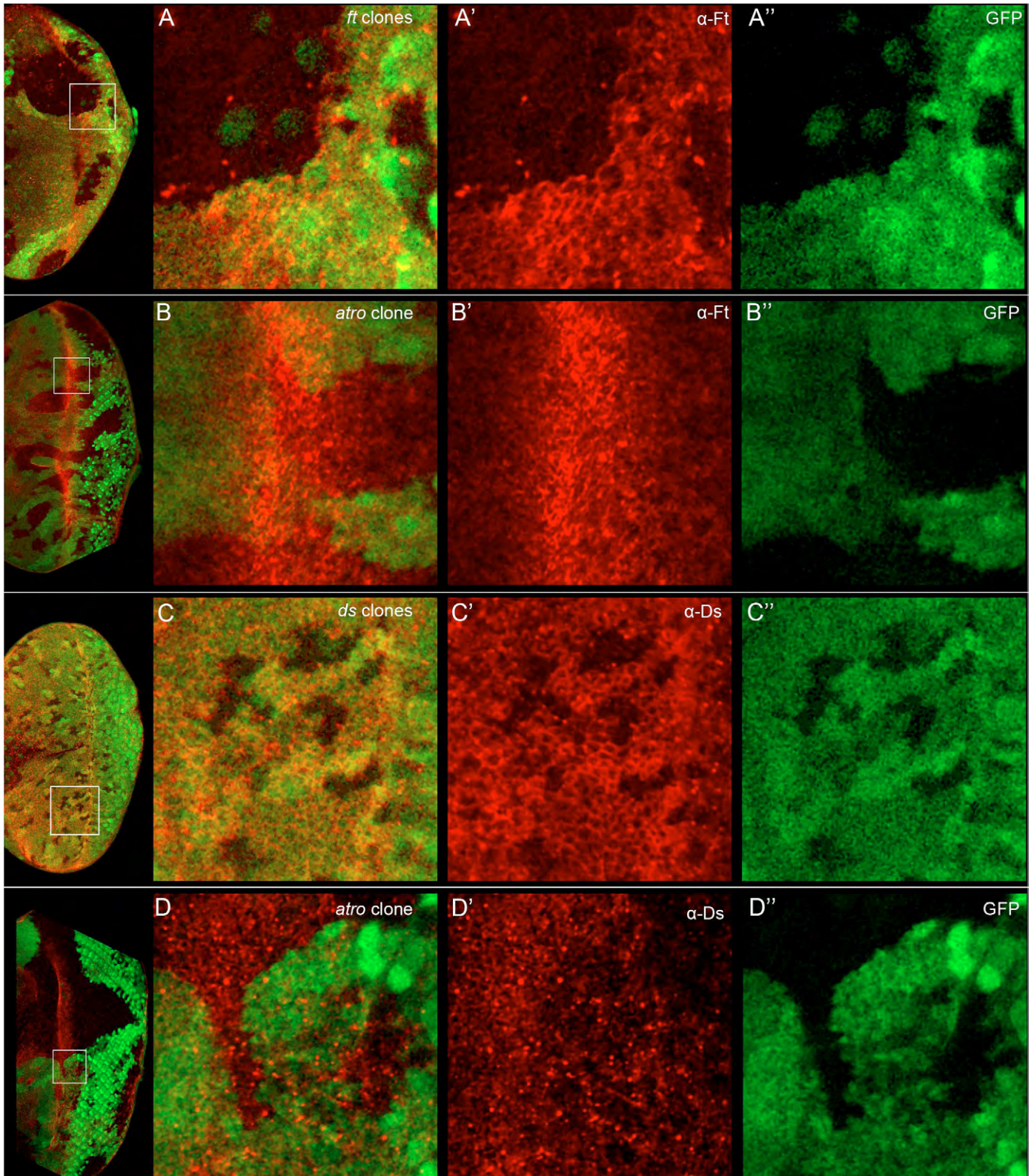
**Fig. S8. Ft and Ds levels and localization are not affected by loss of *atro*.** (**A-A″**) *ft* mutant clones in eye discs, marked by loss of GFP, show loss of α-Ft staining. (**B-B″**) *atro* mutant clones in eye discs, marked by loss of GFP, do not show changes in α-Ft staining. (**C-C″**) *ds* mutant clones in eye discs, marked by loss of GFP, show loss of α-Ds staining. (B-B″) *atro* mutant clones in eye discs, marked by loss of GFP, do not show changes in α-Ds staining.
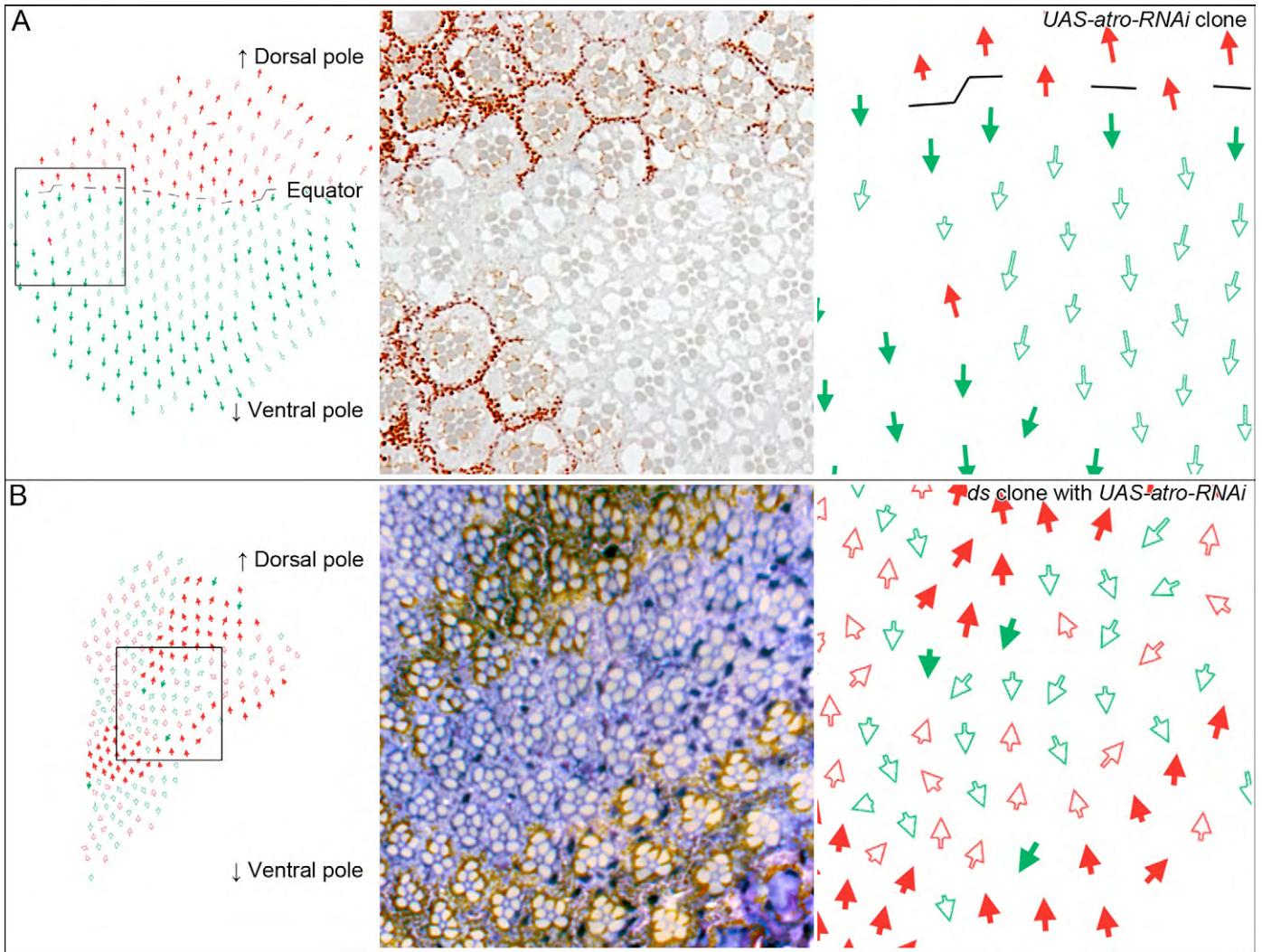
**Fig. S9.** ***ds* clones expressing *UAS-atro-RNAi* cause polar and equatorial polarity reversals.** (**A**) Clones expressing *atro-RNAi* occasionally cause polarity reversals in wild-type ommatidia on the polar side. (**B**) Polarity reversals occur in wild-type ommatidia on the polar and, less frequently, equatorial sides of *ds* clones expressing *atro-RNAi*. No clear rescue or reversal of ommatidial polarity is evident inside the clones.
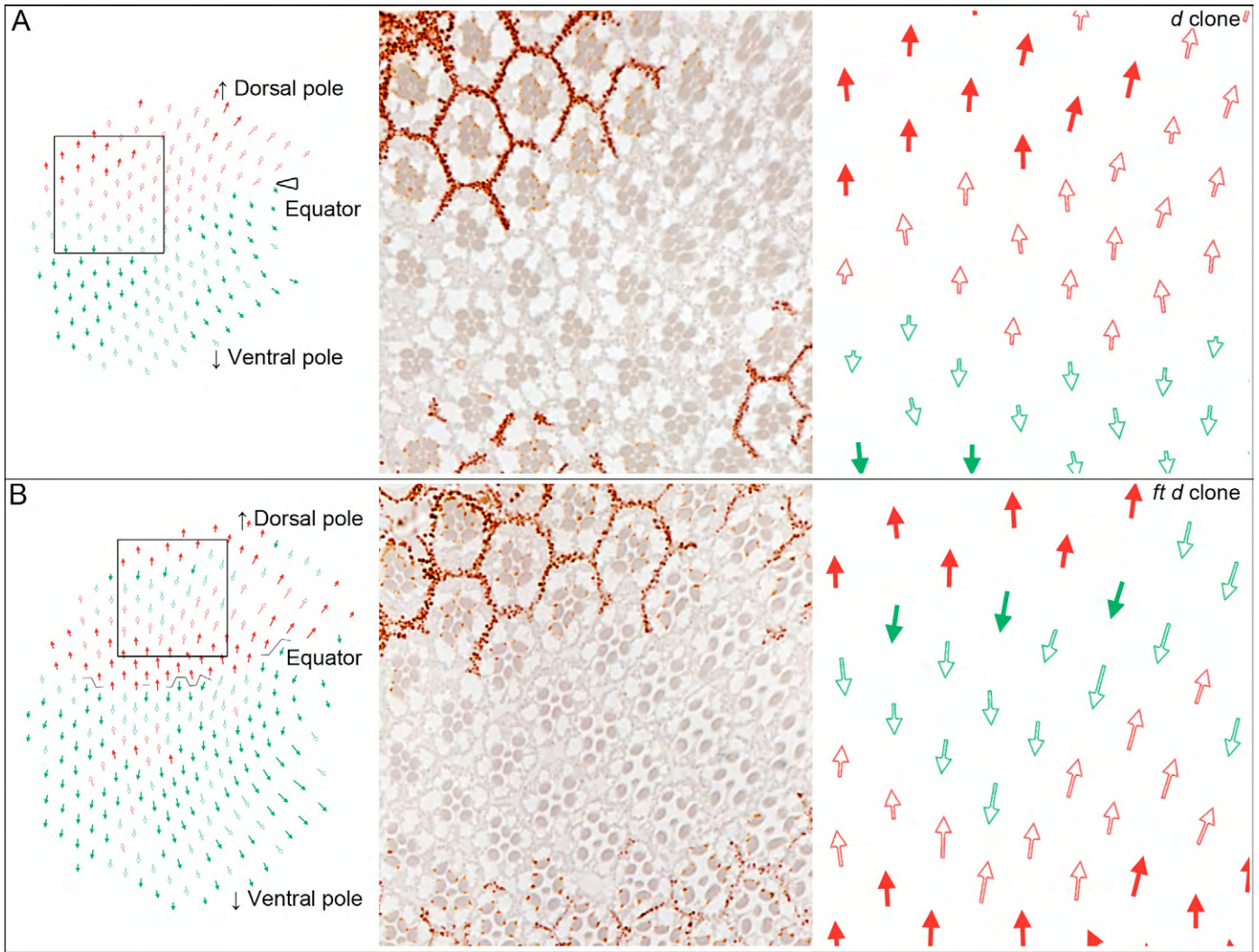
**Fig. S10. _d_ does not regulate PCP in the eye.** (**A**) _d_ mutant clones do not disrupt polarity in the eye. As a clone overlaps the equator in this section, the position of the equator is not marked directly on the eye, but is indicated by the arrowhead. (**B**) _ft d_ double mutant clones affect polarity inside and outside clones similarly to _ft_ mutant clones.
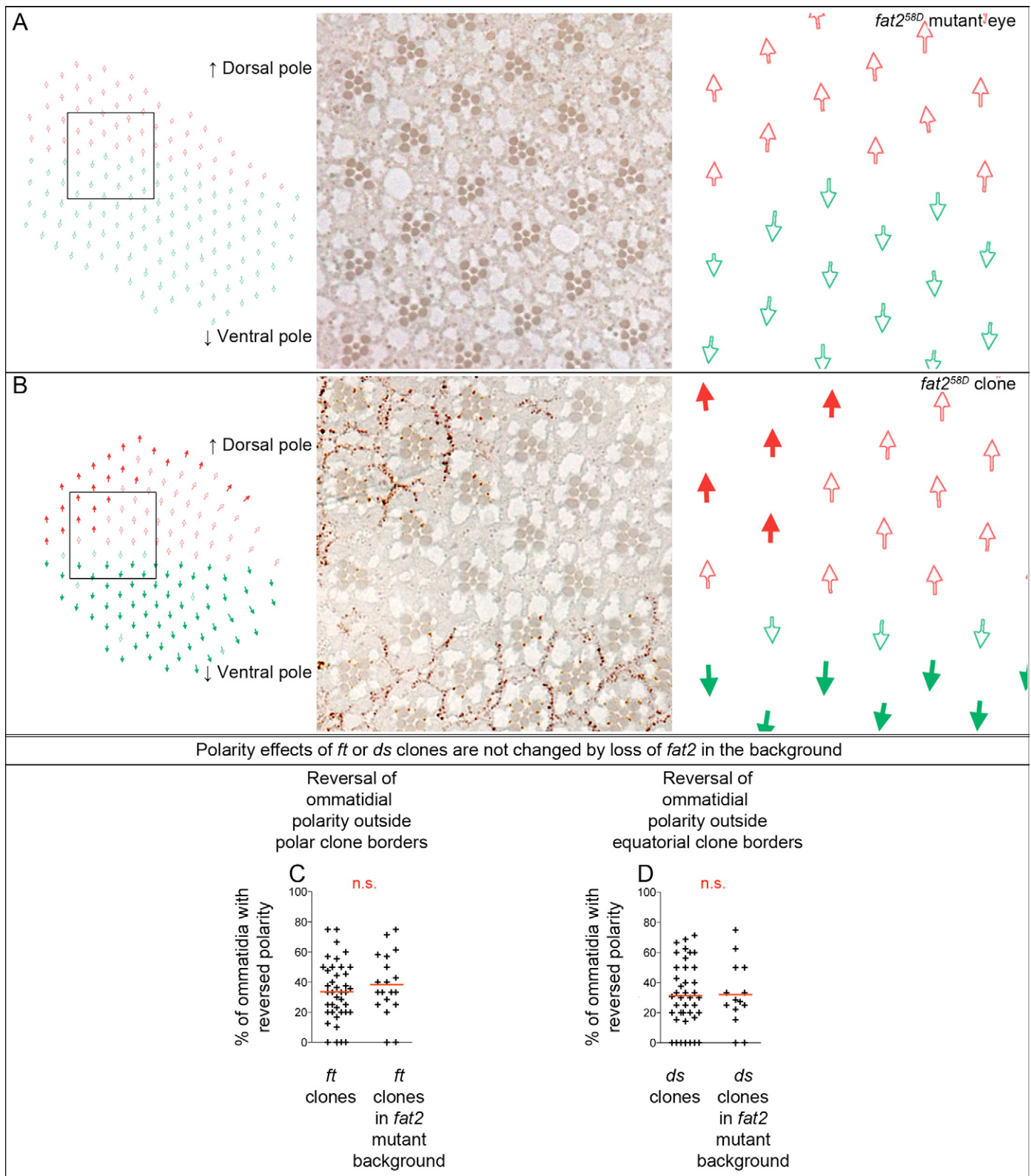
**Fig. S11. *fat2* does not regulate PCP in the eye.** (**A**) A *fat2* mutant eye. Polarity is normal. (**B**) A *fat2* mutant clone, marked by absence of pigment. No changes in polarity are observed inside or outside the clone. (**C**) *ft* mutant clones in a wild-type background do not differ in strength of polarity reversals outside clones from *ft* mutant clones in a *fat2* mutant background. (**D**) *ds* mutant clones in a wild-type background do not differ in strength of polarity reversals outside clones from *ds* mutant clones in a *fat2* mutant background.
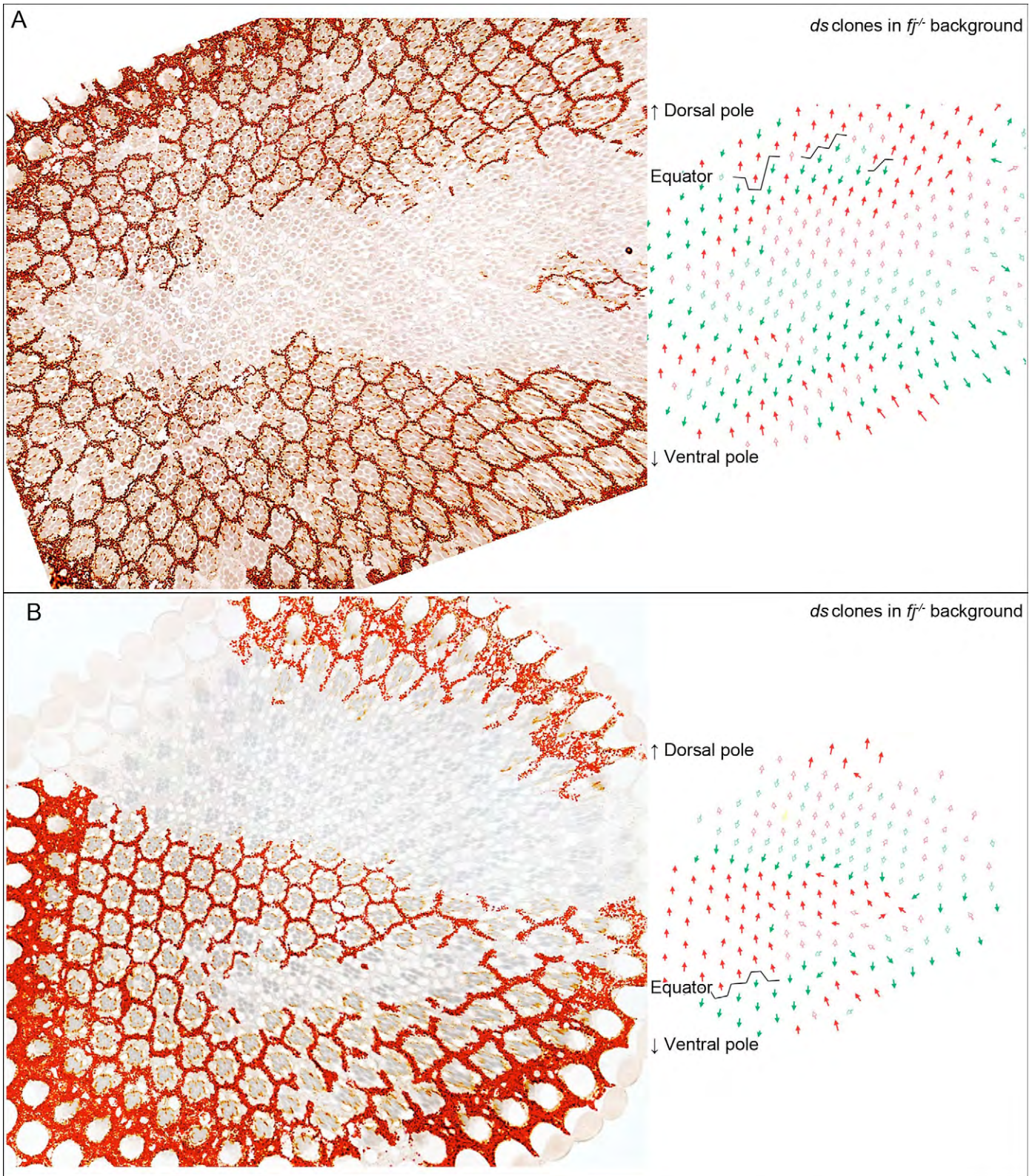
**Fig. S12. Loss of *fj* strengthens *ds* clonal polarity reversals.** *ds⁻* clones generated in a *fj⁻* mutant background show extensive reversal of polarity outside clones, and also reversal and rescue of polarity inside clones, which are missing both *ds* and *fj* gradients.
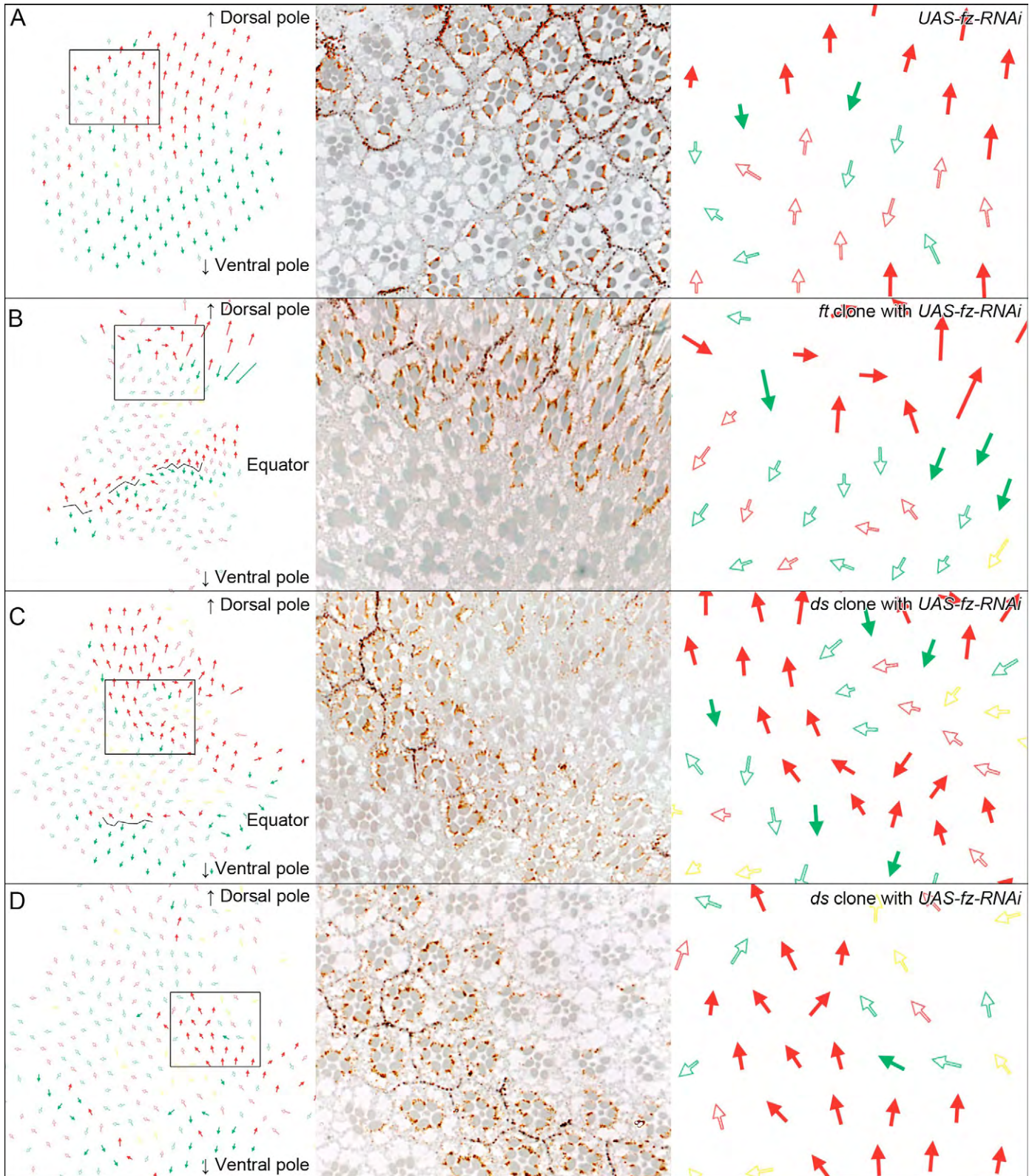
**Fig. S13. *ft* or *ds* clones expressing *UAS-fz-RNAi* cause polar polarity reversals.** (**A**) Clones expressing *fz-RNAi* cause frequent polarity reversals inside the clone, and occasional reversals in wild-type ommatidia on outside the polar border. (**B**) *ft* clone expressing *fz-RNAi*. There is frequent polarity reversal outside the polar side, and polarity inside clones is disrupted to a greater degree than with *ft* clones, with many more misrotated and symmetrical ommatidia. (**C**,**D**) *ds* clones expressing *fz-RNAi*. There is frequent polarity reversal outside the polar side but only rarely outside the equatorial side of these clones. Furthermore, reversals outside the equatorial side are often associated with misrotation. Polarity inside clones is disrupted to a greater degree than with *ds* clones, with many more misrotated and symmetrical ommatidia.

## Table S1. Quantification and comparison of Ft-Ds polarity effects

| # | Figure | Clone | Polarity effect | Number of clones | Number of ommatidia | Statistical significance |
|---|--------|-------|-----------------|------------------|---------------------|--------------------------|
| 1 | 2C, 7A | *ft*⁻ | 33.58% polar reversal | 40 | 331 | |
| 2 | 2G | *ft*⁻ interior – polar side | 88.79% reversal | 36 | 153 | Different to random polarity, *P*<0.0001 |
| 3 | 2H | *ft*⁻ interior – equatorial side | 92.96% rescue | 32 | 128 | Different to random polarity, *P*<0.0001 |
| 4 | 2D | *ft*⁻ – DV size effect | Correlation: *r*=0.0028 | 36 | 274 | No, *P*=0.9872 |
| 5 | 2E | *ft*⁻ – DV position effect | Correlation: *r*=−0.083 | 37 | 282 | No, *P*=0.6266 |
| 6 | 2F | *ft*⁻ – parallel border | 43.96% polar reversal | 36 | 215 | |
| 7 | 2F | *ft*⁻ – slanted border | 13.27% polar reversal | 28 | 107 | Different to #6, *P*<0.0001 |
| 8 | 7C | FtΔECD expression | 1.563% polar reversal | 16 | 81 | |
| 9 | 7D | *ft*⁻ with FtΔECD expression | 26.39% polar reversal | 13 | 71 | Not different to #1, *P*=0.3086 |
| 10 | 7B | *ft*⁻ in *fj*⁻ background | 62.59% polar reversal | 9 | 65 | Different to #1, *P*=0.0003 |
| 11 | 7E | *Fz*-RNAi expression | 3.667% polar reversal | 10 | 58 | |
| 12 | 7F | *ft*⁻ with *fz*-RNAi expression | 40.24% polar reversal | 7 | 45 | Not different to #1, *P*=0.4428 |
| 13 | | *d*⁻ | 1.818% polar reversal | 11 | 45 | |
| 14 | 7G | *ft*⁻ *d*⁻ | 31.53% polar reversal | 19 | 127 | Not different to #1, *P*=0.7153 |
| 15 | 3B, 7H | *ds*⁻ | 31.45% equatorial reversal | 40 | 355 | |
| 16 | 3F | *ds*⁻ interior – polar side | 95.37% rescue | 36 | 153 | Different to random polarity, *P*<0.0001 |

| 17 | 3G | *ds⁻* interior – equatorial side | 65.86% reversal | 29 | 179 | Different to random polarity, *P*=0.0046 |
|---|---|---|---|---|---|---|
| 18 | 3C | *ds⁻* – DV size effect | Correlation: *r*=0.34 | 27 | 221 | No, *P*=0.0872 |
| 19 | 3D | *ds⁻* – DV position effect | Correlation: *r*=0.46 | 33 | 293 | Yes, *P*=0.0073 |
| 20 | 3E | *ds⁻* – parallel border | 30.64% equatorial reversal | 37 | 284 | |
| 21 | 3E | *ds⁻* – slanted border | 41.55% equatorial reversal | 13 | 71 | Not different to #20, *P*=0.2278 |
| 22 | 7J | DsΔECD expression | 4.359% equatorial reversal | 26 | 169 | |
| 23 | 7K | *ds⁻* with DsΔECD expression | 47.60% equatorial reversal | 18 | 120 | Different to #15, *P*=0.0230 |
| 24 | 7L | *ft⁻* with DsΔECD expression – polar border | 40.73% polar reversal | 7 | 71 | Not different to #1, *P*=0.2757 |
| 25 | 7L | *ft⁻* with DsΔECD expression – equatorial border | 0% equatorial reversal | 11 | 92 | N/A |
| 26 | 7M | *ds⁻ ft⁻* with DsΔECD expression – polar border | 6.250% polar reversal | 8 | 42 | Not different to #31, *P*=0.3543 |
| 27 | 7M | *ds⁻ ft⁻* with DsΔECD expression – equatorial border | 0% equatorial reversal | 11 | 72 | N/A |
| 28 | 7I | *ds⁻* in *fj⁻* background | 68.07% equatorial reversal | 23 | 112 | Different to #15, *P*<0.0001 |
| 29 | 7N | *ds⁻* with *fz*-RNAi expression – polar border | 36.41% polar reversal | 14 | 84 | |
| 30 | 7N | *ds⁻* with *fz*-RNAi expression – equatorial border | 4.177% equatorial reversal | 15 | 114 | Different to #15, *P*<0.0001 |
| 31 | 4B, 7O | *ds⁻ ft⁻* | 2.987% polar reversals | 40 | 288 | Different to #1, *P*<0.0001 |
| 32 | 4F | *ds⁻ ft⁻* interior – polar side | 38.42% rescue | 27 | 112 | Not different to random polarity, *P*=0.0844 |
| 33 | 4G | *ds⁻ ft⁻* interior – equatorial side | 72.70% rescue | 30 | 195 | Different to random polarity, *P*<0.0001 |
| 34 | 4C | *ds⁻ ft⁻* – DV size effect | Correlation: *r*=0.11 | 38 | 277 | No, *P*=0.5171 |

| 35 | 4D | *ds⁻ ft⁻* – DV position effect | Correlation: *r*=0.36 | 36 | 267 | No, *P*=0.0335 |
|----|------|------|------|----|-----|------|
| 36 | 4E | *ds⁻ ft⁻* – parallel border | 3.356% polar reversals | 36 | 211 | |
| 37 | 4E | *ds⁻ ft⁻* – slanted border | 0.5348% polar reversals | 17 | 77 | Not different to #36, *P*=0.1114 |
| 38 | 7P | *ds⁻ ft⁻* in *fj⁻* background | 15.73% polar reversals | 6 | 43 | Different to #31, *P*=0.0004 |
| 39 | 7Q | *ds*-RNAi expression | 47.61% equatorial reversals | 4 | 40 | |
| 40 | 6C, 7R | *Atro⁻* | 17.10% polar reversals | 38 | 362 | Different to #1, *P*=0.0003 |
| 41 | 6D | *atro⁻* – DV size effect | Correlation: *r*=−0.11 | 38 | 362 | No, *P*=0.5265 |
| 42 | 6E | *atro⁻* – DV position effect | Correlation: *r*=−0.39 | 35 | 314 | Yes, *P*=0.0200 |
| 43 | 6F | *atro⁻* – parallel border | 18.65% polar reversals | 34 | 302 | |
| 44 | 6F | *atro⁻* – slanted border | 8.044% polar reversals | 14 | 66 | Not different to #43, *P*=0.0795 |
| 45 | 7S | *atro⁻* in *fj⁻* background | 54.65% polar reversals | 13 | 121 | Different to #40, *P*<0.0001 |
| 46 | 7T | *atro*-RNAi | 0.4630% polar reversals | 9 | 69 | |
| 47 | 7U | *ds⁻* with *atro*-RNAi expression– polar border | 10.15% polar reversals | 29 | 168 | Different to #46, *P*=0.0333 |
| 48 | 7U | *ds⁻* with *atro*-RNAi expression – equatorial border | 3.627% equatorial reversals | 44 | 302 | Different to #15, *P*<0.0001 |